Aus der Medizinischen Klinik und Poliklinik IV

Klinik der Universität München

Direktor: Prof. Dr. Martin Reincke

The immune-modulating effects of PFKFB3 inhibition in a syngeneic ovarian cancer model

Dissertation zum Erwerb des Doktorgrades der Medizin

an der Medizinischen Fakultät

der Ludwig-Maximilians-Universität zu München

vorgelegt von

ASSJA ALEXEEVNA JESKE

aus Petrosawodsk, Russland

2023

Mit Genehmigung der Medizinischen Fakultät

der Universität München

Berichterstatter:	Prof. Dr. Ralf Schmidmaier
Mitberichterstatter:	Prof. Dr. Fabian Trillsch
	PD Dr. Markus Moser
Mitbetreuung durch den promovierten Mitarbeiter:	Matt Block, MD Ph.D.
Dekan:	Prof. Dr. Thomas Gudermann

Tag der mündlichen Prüfung: 15.06.2023

Meiner unerschrockenen Mutter in Dankbarkeit

Table of Contents

I. List of abbreviations

%	percent
°C	degrees Celsius
2DG	2-deoxyglucose
ATP	adenosine triphosphate
BSA	bovine serum albumin
Cnrl	control (group)
CO_2	carbon dioxide
CTL	cytotoxic T lymphocyte
CTV	CellTrace Violet
ddH_2O	deionized water
DMSO	dimethyl sulfoxide
EDTA	ethylenediaminetetraacetic acid
ELISA	enzyme-linked immunosorbent assay
EOC	epithelial ovarian cancer
F2,6BP	fructose-2,6-bisphosphate
FBS	fetal bovine serum
FVB	inbred mouse colony for the Fvb1 gene (in–house), immune competent
GAPDH	glycerinaldehyd-3-phosphat-dehydrogenase
H_2O	water
HEPES	4-(2-hydroxyethyl)-1-piperazineethanesulfonic acid
HPF	high power field
hrs	hours
i.e.	id est
i.p.	intraperitoneal
IC	inhibitory concentration
IFN-ɣ	interferon-ɣ
IHC	immunohistochemistry
IL-	interleukin-
mAbs	mouse antibodies
ml	milliliters
mM	millimole

MDSc	myeloid-derived suppressor cell
mins	minutes
MTT	3-(4,5-dimethylthiazol-2-yl)-2,5- diphenyltetrazolium bromide
nm	nanometre
NTC	not treated control
OC	ovarian cancer
OXPHOS	oxidative phoshorylation
p-	phospho-
PCNA	proliferating-cell-nuclear-antigen
PBS	phosphate buffered saline
PFK-1	6-phosphofructo-1-kinase
PFKFB3	6-Phosphofructo-2-Kinase/Fructose-2,6-Biphosphatase 3
rpm	revolutions per minute
RT	room temperature
SD	standard deviation
SDS	sodium dodecyl sulfate
t-	total
TBS	tris buffered saline
TBST	tris buffered saline with Tween 20
TIL	tumor infiltrating lymphocytes
TME	tumor microenvironment
vs.	versus
µl	microliters
µM	micromole

II. List of figures

III. Introduction

III.1 Ovarian cancer – statistical data and overview

At present, ovarian cancer not only causes a third of all gynecological malignancies but has also proven to be the most lethal tumor of the female reproductive system. According to the most recent statistics, approximately 7.300 new cases of ovarian cancer and an estimated 5.326 deaths have been reported in Germany in the year 2018 (Zentrum für Krebsregisterdaten, 2021). Due to the clinical presentation of the disease, the majority of women with ovarian cancer (est. 75%) are diagnosed at a later stage (stadium III-IV). The symptomless disease progression results in significantly decreased chances of survival and remission in these patients (Zentrum für Krebsregisterdaten, 2021). Globally, the number of new cases has reached 313.959 with 207.252 deaths in 2020 (Sung et al., 2021).

The most common type of ovarian cancer is the epithelial ovarian cancer (EOC). The World Health Organization has established further classification of EOC into several categories according on the histological type: serous, endometrioid, mucinous and clear-cell carcinomas, as well as the transitional, mixed and the undifferentiated type (Kaku et al., 2003). Despite numerous distinctive features in disease origin, morphology, clinical progression and expected prognosis, all types are treated as one single entity (Bai et al., 2016; Kossaï, Leary, Scoazec, & Genestie, 2018; Romero, Leskelä, Mies, Velasco, & Palacios, 2020).

The current standard of care remains cytoreductive surgery followed by platinum- and taxane-based combination chemotherapy (Burges & Schmalfeldt, 2011; A. J. Li & Karlan, 2003; Pignata et al., 2011). Around 80-90% of patients respond to first-line therapy, however, studies show a 50-75% probability of relapse within 18 months (Herzog, 2004).

The deadly nature of EOC arises from its` rapid, asymptomatic growth and delayed primary diagnosis as well as subtype heterogeneity and high probability of relapse. For patients diagnosed with stages III or IV disease, the 5-year survival rate drops below 40% (Torre et al., 2018). In an effort to improve patients' outcome, recent clinical trials have incorporated antiangiogenics such as bevacizumab into existing chemotherapy regimens. However, no definitive increase in overall survival could

be observed, suggesting that conventional therapies have reached a plateau (Odunsi, 2017).

Consequently, new strategies are needed to ensure a more effective treatment regime and improvement in patient outcome. New avenues for the development of alternative therapies have been opened due to recent progress in understanding cancer cell metabolism.

III.2 Cancer cell metabolism and the Warburg effect

Under physiological conditions, the primary aerobic energy supply for healthy cells derives in the form of ATP from mitochondrial oxidative phosphorylation (Reutter, Emons, & Gründker, 2013). In some cases, cells are also able to produce energy anaerobically by fermenting glucose. The initial metabolic pathway for both processes is glycolysis, which results in the production of pyruvate from glucose and is regulated by 6-phosphofructo-1-kinase (PFK-1). Under aerobic conditions, pyruvate fuels the tricarboxylic acid cycle in the mitochondria, which creates high levels of ATP, citrate and CO_2 - contrary to anaerobic conditions, where pyruvate is turned into lactate and a smaller yield of ATP in the cytosol (Icard et al., 2018).

Cancer cells express an increased demand for energy in order to fulfill their bioenergetics and biosynthetic demand to support rapid proliferation, resulting in a metabolic transformation known as the Warburg effect. Otto Warburg and Carl and Gerty Cori demonstrated an increased glucose absorption by tumors as compared to benign tissues of origin in 1927 (Cori & Cori, 1925; Warburg, Wind, & Negelein, 1927). Furthermore, Warburg has shown, that proliferating cancer cells selectively utilize glycolysis and produce lactate, even if sufficient oxygen is available (Warburg, 1956). There are several ways, in which the process of “aerobic glycolysis” has been shown to be essential for cancer cell survival. First, it provides a quick way to generate ATP, thus ensuring high cellular proliferation flexibility. Second, metabolic compounds for the biosynthesis of complex molecules, such as amino acids and lipids emerge as the byproduct (Ma et al., 2018). Third, generating energy through higher rates of glycolysis relative to oxidative phosphorylation also reduces reactive oxygen species-related damage (Lu, Chen, & Zhu, 2017). This shift in cellular

metabolism is, in fact, a direct consequence of reprogramming regulated by oncogenes and tumor suppressor genes and is recognized today as a "hallmark of cancer" (Ganapathy-Kanniappan & Geschwind, 2013; Jang, Kim, & Lee, 2013).

The glycolytic pathway presents various possibilities for targeted therapy in cancer cells. Many inhibitors of glycolytic key enzymes such as hexokinase 2 (Del Bufalo et al., 1996), phosphofructokinase 2 (Mondal et al., 2019), pyruvate kinase (Pouessel et al., 2008), lactate dehydrogenase A (Le et al., 2010) and pyruvate dehydrogenase kinase (Wong, Huggins, Debidda, Munshi, & De Vivo, 2008) have shown anti-tumor effects in preclinical studies.

We have focused our investigation on the allosteric enzyme PFKFB3 which not only is a viable target in OC per se but also integrates glycolysis with immune differentiation and its effects on the tumor microenvironment.

III.3 Expression and inhibition of PFKFB3

PFKFB3 belongs to a group of four bifunctional isoenzymes (PFKFB1-4), which regulate the transformation between fructose-6-phosphate and fructose-2,6-bisphosphate in the process of glucose metabolism (Bando et al., 2005). It is an essential molecule in controlling glycolysis; due to its stronger kinase activity than phosphatase activity, it promotes the synthesis of fructose-2,6-bisphosphate - a key allosteric regulator of glycolysis that stimulates the activity of 6-phosphofructo-1-kinase (PFK-1), which is a rate-limiting enzyme and the most important check point in mammalian glycolysis. Subsequently, the glycolysis flux is increased (Lu et al., 2017). The overexpression of PFKFB3 is markedly higher in rapid proliferation cells and has been documented in several tumor types including ovarian cancers (Atsumi et al., 2002; Yalcin, Clem, et al., 2009). Many studies have reported a correlation between PFKFB3 expression level and the grade of tumor aggressiveness, indicating the crucial role these enzymes play in carcinogenesis (Clem et al., 2008; Kocemba, DuljDska-Litewka, WojdyBa, & Q kala, 2016).

Recent discoveries related to the role of PFKFB3 in tumorigenesis and cancer progression have identified their inhibitors as potential therapeutics that could play a key role in future cancer treatment (Lu et al., 2017). PFK-158, a novel, potent and selective molecule inhibitor of PFKFB3, has shown promising results in inhibiting tumor growth in gynecologic cancers (Mondal et al., 2019; Xiao et al., 2021).

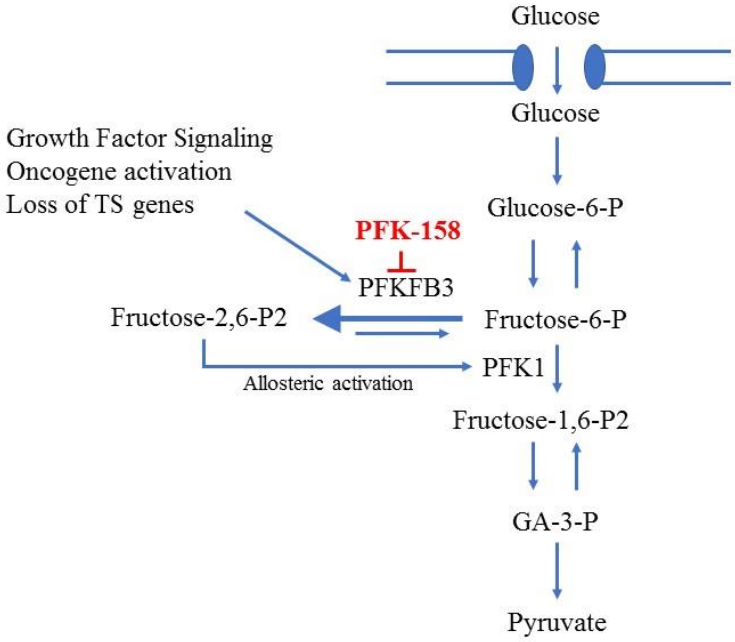

Fig. 1: PFKFB3 (selectively inhibited by PFK-158) controls the conversion of fructose-6-phosphate to and from fructose-2,6-bisphosphate, a key activator of phosphofructokinase-1 (PFK1).

III.4 The role of glucose metabolism in immune signalling

Immune cells use nutrients in their direct environment through cellular metabolism to meet their energy requirements for basic upkeep (such as growth, protein synthesis and ion integrity) as well as specific immune functions. The levels of ATP consumption vary depending on the performed task. Cytokinesis, cell migration, antigen processing and presentation, phagocytosis, lymphocyte activation and synthesis of chemokines and antibodies require higher levels of ATP when the cells enter a state of high biochemical activity after stimulation (Krauss, Brand, & Buttgereit, 2001).

Both CD8+ cytotoxic T cells and CD4+ T helper cells play a key effector role in anti-tumor immunity (Lai, Jeng, & Chen, 2011). Naïve T rely on catabolic metabolism, meaning they interchangeably break down glucose, amino acids and lipids for ATP generation much like cells from normal tissues. After antigenic stimulation, however, T cells rapidly undergo an anabolic switch to increased glycolysis and preferably ferment glucose to fulfil their energy demands, despite sufficient oxygen being present to allow for mitochondrial phosphorylation (T. Wang, Marquardt, & Foker, 1976). The Warburg effect is hence a phenomenon not only observed in oncogenesis but is also part of the physiological T cell proliferation process. One glucose molecule converted into pyruvate results in a net production of two ATP molecules. At first, it may seem implausible, that activated T cells would increasingly exploit a comparatively insufficient process to generate energy. An explanation for this metabolic conversion can be found in the anabolic character of aerobic glycolysis. This process leaves amino acids and fatty acids intact and creates lactate, all of which can be integrated into cellular components, offering a decisive advantage through efficient and rapid cell expansion in the fight against a pathogen (Fox, Hammerman, & Thompson, 2005; Vander Heiden, Cantley, & Thompson, 2009). Furthermore, this rapid process occurs independently of mitochondrial function (Palmer, Ostrowski, Balderson, Christian, & Crowe, 2015).

Lymphocyte activation has been associated with increased concentration of fructose-2,6-bisphosphate (Simon-Molas et al., 2018), which is in turn mediated by PFKFB3. Inhibition of PFKFB3 was demonstrated to suppress T cell immunity in vivo (Telang et al., 2012). However, not all lymphocyte subset populations commit to aerobic glycolysis after undergoing activation to the same extent. It is important to note that the commitment to a certain metabolic pathway is dependent on the specific cell function, a phenomenon best observed in the CD4+ T cells subsets. While effector T cells (Th1/Th2) and Th17 cells mostly depend on aerobic glycolysis, regulatory T cells and memory T cells utilize fatty acid oxidation for energy production (Michalek et al., 2011).

III.5 Link between glycolysis and anti-tumor immunity

Contradictory to earlier theories, that cancer could not cause an immune reaction, multiple studies have later underlined the importance of the immune system in the initiation and progression of ovarian cancer (Baci et al., 2020; Gavalas, Karadimou, Dimopoulos, & Bamias, 2010; Lai et al., 2011). More specifically, both innate and adaptive immunity are involved in eliciting anti-tumor immunity, marked by complex interactions of cancer cells, effector cells and cytokines present in the tumor microenvironment (Cândido et al., 2013; Gavalas et al., 2010). A process that describes the dynamic interaction between the immune system and cancer is labelled as "immunoediting". It takes place in most cancer types including OC and is divided into three stages: elimination, equilibrium, and finally escape from immune surveillance (Dunn, Old, & Schreiber, 2004; O'Donnell, Teng, & Smyth, 2019).

Elimination is mainly achieved by CD8+ cytotoxic T lymphocytes (CTL), the primary mediators of anti-tumor immune response, which are able to directly induce tumor cell death (Tang et al., 2020; R. F. Wang, 2001; Wieder, Braumüller, Kneilling, Pichler, & Röcken, 2008). Recent studies confirmed that CD8+ T cell infiltration is associated with a favourable prognosis in OC patients (Hamanishi et al., 2011; Hwang, Adams, Tahirovic, Hagemann, & Coukos, 2012; W. Wang, Zou, & Liu, 2018). Together with preclinical data, these findings indicate that strengthening the host immune system may help achieve a more substantial tumor reduction. A possible synergistic effect with other therapies is subject to further investigation.

Despite a well-established development of an anti-tumor immune response, growing evidence suggests, that cancer cells can escape destruction by immunosuppressive signalling in the tumor microenvironment (Gavalas et al., 2010). Thus, its' composition appears crucial as a potential target for OC therapy. For instance, such a target is represented by Th17 cells, which have been identified as immunosuppressive mediators and therefore promote tumor development in various cancers (He et al., 2010). Th17-derived IL-17 production in the ascites has been shown to enhance tumor growth via the TNF-α signalling pathway (Charles et al., 2009). Moreover, patients diagnosed with ovarian serous cystadenocarcinoma expressed higher levels of serum IL-17 compared to healthy individuals (Malekzadeh, Dehaghani, Ghaderi, & Doroudchi, 2013). Recently, it has been shown

that the differentiation of Th17 cells is induced by elevated levels of the oncogenic protein HIF1α, a potent activator of the glycolytic pathway and transcription factor for PFKFB3 (Dang et al., 2011). Therefore, PFKFB3 integrates glycolysis with immune differentiation and its effects on the tumor microenvironment.

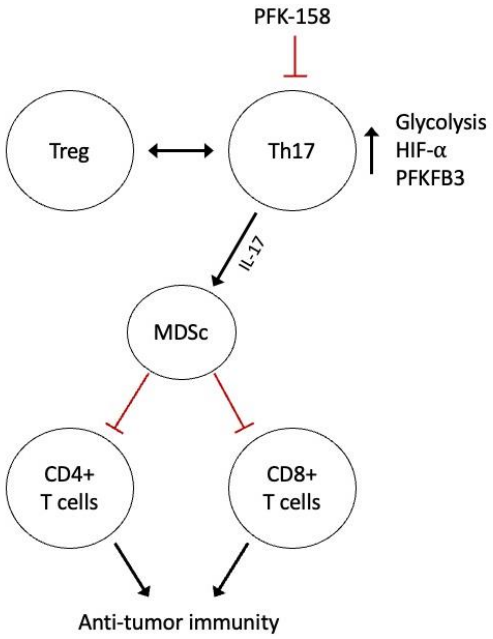

Fig. 2: Th17-derived IL-17 promotes tumor development through the induction of myeloid-derived suppressor cells (MDSc) in ovarian cancer.

Understanding the cause-and-effect relationship between glycolytic metabolism and the T cell-mediated immune response is currently a subject of intense scientific interest. While the action of PFKFB3 inhibition in modulating the glycolytic pathway is well documented, there are no reports on whether PFK-158 treatment affects T cell function and differentiation through metabolic alterations and the way these changes influence the anti-tumor immune response and the constitution of the tumor microenvironment in ovarian cancer.

IV. Study objective

The objective of this study is to determine the immune-modulating effects of PFK-158, a novel glycolytic inhibitor that has currently been studied in clinical trial in syngeneic ovarian cancer models (National Library of Medicine (NCT02044861), January 2014 -). PFKFB3 controls the transformation of fructose-6-phosphate to and from fructose-2,6-bisphosphate, a key activator of the glycolytic enzyme phosphofructokinase-1 (PFK-1). In unpublished data it has recently been demonstrated that Th17 cells, which play a crucial role in mediating immunogenicity of various cancers including OC, show elevated activity of PFKF3B, resulting in a promising new therapy target. While the action of PFK-158 in modulating the glycolytic pathway is well documented, there are no reports in ovarian cancer on whether PFK-158 treatment affects the immune system and how treatment changes the composition of the tumor microenvironment.

1. Does PFKFB3 inhibition reduce cancer cell proliferation *in vitro* and tumor burden *in vivo*?

First, the effect of PFKFB3 inhibition on STOSE cells was studied *in vitro*. After cytoreductive properties of PFK-158 were established, the effect of single treatment with the glycolytic inhibitor on tumor burden and ascites volume was monitored in a syngeneic OC model *in vivo*.

2. Does PFKFB3 inhibition modulate signals that influence immune cell function and proliferation *ex vivo*?

Second, the ability of CD4+ cells to differentiate, proliferate and secrete cytokines in the presence and absence of PFK-158 was assessed *ex vivo*. Cytokines, which have been identified as prognostic factors for OC progression (IL-4, IL10, IL-17 and IFNɣ) as well as proliferation of CD4+ T cells under the influence of PFK-158 will be examined in a dose-dependent manner. The primary analyses are dedicated to understanding the impact of PFK-158 on the function of immunostimulating and immunosuppressing effector cells *ex vivo*.

3. Does PFKFB3 inhibition modulate the immune response *in vivo*?

Third, $15x10^6$ STOSE cells were injected intraperitoneally (i.p.) into female FVB mice in groups of 8 and treated with 60mg/kg of PFK-158 every third day. Treatment was initiated on day 35 when smaller tumor masses could be palpated. At endpoint, following tissues were collected – plasma, ascites, tumor burden and spleen.

Using immunohistochemistry, ELISA and flow cytometry, we determined the effect of PFK-158 treatment on the immune profile measured in cytokine expression and specific lymphocyte populations *in vivo*.

V. Materials and Methods

V.1. Materials

V.1.1 Cell lines

M505	Gifted by Barbara Vanderhyden, PhD, Ottawa Hospital Research Institute, Ottawa, Canada
STOSE	Gifted by Barbara Vanderhyden, PhD, Ottawa Hospital Research Institute, Ottawa, Canada

V.1.2 Cell culture media

M505/STOSE cells	
MEM (Minimum Essential Medium) α 1X	Gibco™ by life technologies, Invitrogen, Grand Island, NY, USA
FBS (Fetal Bovine Serum)	Biowest, Riverside, MO, USA
Recombinant Mouse EGF Protein (0.1 mg/ml)	R&D Systems Inc., Minneapolis, MN, USA
ITSS (Insulin-Transferrin-Sodium Selenite) 1000X	Roche, Indianapolis, IN, USA
Gentamicin (10 mg/ml)	Sigma-Aldrich, St. Louis, MO, USA
Penicillin/Streptomycin 100X	Gibco™ by life technologies, Invitrogen, Grand Island, NY, USA
Isolated T cells	
RPMI-1640	Mediatech Inc., Herndon, VA, USA
HEPES Buffer 25 mM	Mediatech Inc., Herndon, VA, USA
MEM Non-Essential Amino Acids 0.1 mM	Gibco™ by life technologies, Invitrogen, Carlsbad, CA, USA
Sodium Bicarbonate 1.5 g/L	Gibco™ by life technologies, Invitrogen, Carlsbad, CA, USA
Sodium Pyruvate 1 mM	Gibco™ by life technologies, Invitrogen, Carlsbad, CA, USA
L-Glutamine 2 mM	Gibco™ by life technologies, Invitrogen, Carlsbad, CA, USA
2- Mercaptoethanol 50 mM	Gibco™ by life technologies, Invitrogen, Carlsbad, CA, USA

V.1.3 Labware and materials

4-Well Chamber Slides	Thermo Fisher Scientific, Rockford, IL, USA
70 µm Nylon Cell Strainer	BD Falcon, Franklin Lakes, NY, USA
8-Channel Micropipette	Thermo Fisher Scientific, Rockford, IL, USA
6-/96-Well Plates	Corning Life Sciences, Big Flats, NY, USA
Cell Culture Flasks 25 cm^2/150cm^2	BD Falcon, Franklin Lakes, NY, USA
Gel-loading Tips	Thermo Fisher Scientific, Rockford, IL, USA
Gilson Micropipette	Thermo Fisher Scientific, Rockford, IL, USA
Micropoint Pipette Tips	Thermo Fisher Scientific, Rockford, IL, USA
Polypropylene Specimen Containers	Kendall, Tyco Healthcare, Mansfield, MA, USA
Polystyrene Round-Bottom Tubes, 5 ml	BD Falcon, Franklin Lakes, NY, USA
Serological Glass Pipette 5/10ml	BD Falcon, Franklin Lakes, NY, USA
Tissue Embedding Cassettes	Leica Biosystems, Nussloch, Germany

V.1.4 Instruments

Allegra 6R Refrigerated Centrifuge	Beckman Coulter Inc., Brea, CA, USA
Block Heater	Thermo Fisher Scientific, Rockford, IL, USA
Centrifuge IEC Centra CL2	Thermo Scientific, Waltham, MA, USA
CO_2 Incubator	Thermo Scientific, Waltham, MA, USA
Criterion Gel Electrophoresis Cell	Bio-Rad Laboratories, Hercules, CA, USA
Hemacytometer Reichert Bright-Line	Hausser Scientific, Horsham, PA, USA
Light Microscope	Nikon, Melville NY, USA
LS MACS Column (for 1×10^8 cells)	Miltenyi Biotec GmbH, Bergisch Gladbach, Germany
MidiMACS Separator	Miltenyi Biotec GmbH, Bergisch Gladbach, Germany
OdysseyFc Imaging System	LI-COR Biosciences, Lincoln, NE, USA
Orbital Shaker	Scientific Industries, Bohemia, NY, USA
PowerPac Basic 300 V Power Supply	Bio-Rad Laboratories, Hercules, CA, USA
Refrigerated Microcentrifuge	Corning Life Sciences, Big Flats, NY, USA
Spectrophotometer, DU 530	Beckman Coulter, Inc., Brea, CA, USA
Synergy HTX Multi-Mode Reader	Biotek, Winooski, VT, USA

Trans-Blot Turbo Transfer System	Bio-Rad Laboratories, Hercules, CA, USA
Zeiss LSM510 Fluorescence Microscope	Carl Zeiss AG, Oberkochen, Germany

V.1.5 Chemicals, reagents and kits

0.25 % Trypsin-EDTA 1X	Gibco™ by life technologies, Invitrogen, Carlsbad, CA, USA
2DG	Perkin Elmer Inc., Waltham, MA, USA
2-NBDG	Cayman Chemicals, Ann Arbor, MI, USA
3-(4,5-dimethylthiazol-2-yl)-2,5-Diphenyltetrazolium Bromide (MTT)	Thermo Fisher Scientific, Rockford, IL, USA
ACK (Ammonium-Chloride-Potassium) Lysis Buffer	Thermo Fisher Scientific, Rockford, IL, USA
ATP Colorimetric Assay Kit	Biovision, Milpitas, CA, USA
Bovine Serum Albumin Powder	MP Biomedicals, Solon, Ohio, USA
Calcium Chloride	Sigma-Aldrich, St. Louis, MO, USA
$CD8^+/CD4^+$ T Cell Isolation Kit, Mouse	Miltenyi Biotec GmbH, Bergisch Gladbach, Germany
Cell Lysis Buffer 10X	Cell Signaling Technology Inc., Danvers, MA, USA
CellTrace Violet Cell Proliferation Kit	Thermo Fisher Scientific, Waltham, MA, USA
Criterion TGX Stain-Free Precast Gel, 18-Well	Bio-Rad Laboratories, Hercules, CA, USA
Cytofix/Cytoperm Kit	BD Biosciences, San Diego, CA, USA
DMSO (Dimethyl Sulfoxide)	Thermo Fisher Scientific, Rockford, IL, USA
Dulbecco`s PBS (Phosphate-Buffered Saline) 1X	Corning Life Sciences, Big Flats, NY, USA
EDTA	Thermo Fisher Scientific, Rockford, IL, USA
Ethanol	Sigma-Aldrich, St. Louis, MO, USA
Glycerol	Thermo Fisher Scientific, Rockford, IL, USA
Krebs-Ringer Solution, HEPES-Buffered	Thermo Fisher Scientific, Rockford, IL, USA
Mouse IFNɣ/ -IL-4/ -IL-17/ -IL-10 Quantikine® ELISA Kit	R&D Systems, Minneapolis, MN, USA

Neutral Buffered Formalin 10 %	Thermo Fisher Scientific, Rockford, IL, USA
NP-40	Sigma-Aldrich, St. Louis, MO, USA
NuPage LDS Sample Buffer 4X	Novex by life technologies, Invitrogen, Carlsbad, CA, USA
Pageruler Prestained Protein Ladder	Thermo Fisher Scientific, Rockford, IL, USA
PFK-158	Advanced Cancer Therapeutics, Louisville, KY, USA
Protease Inhibitor Cocktail	Sigma-Aldrich, St. Louis, MO, USA
Protein Assay Dye Reagent Concentrate	Bio-Rad, Hercules, CA, USA
Sodium Chloride	Sigma-Aldrich, St. Louis, MO, USA
Tris/Glycine Transfer Buffer 10X	Bio-Rad Laboratories, Hercules, CA, USA
Tris/Glycine/SDS Running Buffer 10X	Bio-Rad Laboratories, Hercules, CA, USA
Tryptan Blue Stain (0.4 %)	Gibco™ by life technologies, Invitrogen, Carlsbad, CA, USA
Tween 20 Detergent	Bio-Rad Laboratories, Hercules, CA, USA

V.1.6 Antibodies

Anti-CD4/-CD25/-CD3/-CD8, monoclonal	eBiosciences, San Diego, CA, USA
Anti-CD8 α, rabbit, monoclonal	Abcam, Waltham, MA, U.S.A
Anti-FOXP3, monoclonal	eBiosciences, San Diego, CA, USA
Anti-GATA3, monoclonal	eBiosciences, San Diego, CA, USA
Anti-mouse CD28, monoclonal	BioXCell, Lebanon, NH, USA
Anti-mouse CD3e, monoclonal	BioXCell, Lebanon, NH, USA
Anti-RORγ(t), monoclonal	eBiosciences, San Diego, CA, USA
Anti-T-bet, monoclonal	eBiosciences, San Diego, CA, USA
GAPDH	Santa Cruz Biotechnology, Dallas, TX, USA
Ki67, rabbit, monoclonal	Cell signaling Technology, Danvers, MA, USA
PCNA	Santa Cruz Biotechnology, Dallas, TX, USA
p-PFKFB3	Custom made by GenScript Inc., Piscataway, NJ, USA
t-PFKFB3	Abcam, Cambridge, UK

V.1.6 Laboratory animals

25 eight week old, female FVB mice were obtained from Jackson Laboratory (Bar Harbor, Maine USA). They were housed with a 12 hours light and 12 hours dark photoperiod and had free access to food and water. The experiments complied with the Institutional Animal Care and Use Committee (IACUC) guidelines at the Mayo Foundation, following approved protocols.

V.2. Methods

V.2.1 Cell culture

An independent isolation of mouse ovarian surface epithelial cell line (M505) was established in 2005 by Gamwell et al (Gamwell, Collins, & Vanderhyden, 2012). Long-term passage of M505 led to spontaneous transformation, the resulting cell line was from that point on labeled STOSE (McCloskey et al., 2014). The STOSE cells syngeneic cancer model resembles high grade serous ovarian cancer in genetic expression, morphological appearance and proliferation rates (McCloskey et al., 2014). Both cell lines were maintained in recommended MOSE media, consisting of MEMα (Invitrogen, Grand Island, NY, USA), supplemented with 4.4 % fetal bovine serum, epidermal growth factor (0.1 mg/ml), and 1 % Insulin-Transferrin-Sodium Selenium (Invitrogen, Grand Island, NY, USA). The antibiotic penicillin and streptomycin (Invitrogen, Grand Island, NY, USA), as well as gentamicin (Sigma-Aldrich, St. Louis, MO, USA) were added to the growth media. All cell lines were grown in a 25 cm^2 tissue culture flask and maintained in humidified incubator at 37°C with 5 % CO_2. Cells were passaged every 3 days. Both cell lines were gifted by Barbara Vanderhyden, PhD, Ottawa Hospital Research Institute, Ottawa, Canada.

Isolated T cells were isolated from FVB-mouse spleens and maintained in recommended media, consisting of RPMI-1640 supplemented with 10 % FBS, 25 mM HEPES Buffer (Mediatech, Herndon, VA, USA), 1.5 g/L sodium bicarbonate, 0.1 mM MEM non-essential amino acids, 1 mM sodium pyruvate, 2 mM L-glutamine and 50 mM 2-mercaptoethanol (Invitrogen, Carlsbad, CA, USA).

V.2.2 T cells isolation and activation

T cells were obtained from healthy FVB mouse spleens by pressing the spleen through a 70 µm nylon cell strainer. The splenocytes were centrifuged at 3000 rpm for 10 minutes and resuspended in 3 ml ACK buffer (Ammonium-Chloride-Potassium) to lyse red blood cells. The remaining cells were then washed with PBS and counted. Single $CD8^+/CD4^+$ T cells were negatively selected via magnetic column separation using the MACS system (Miltenyi Biotec GmbH, Bergisch Gladbach, Germany). MACS cell isolation kits for untouched isolation contain a cocktail of titrated antibodies and MACS Anti-Biotin MicroBeads for indirect magnetic labelling. Counted cells were resuspended in 40 µl buffer solution containing PBS, 0.5 % bovine serum albumin and 2 mM EDTA total cells (reagents provided in the kit, all volumes are given for $1x10^7$ cells). First, 10 µl of Biotin-Antibody cocktail was added, followed by a 5 minutes incubation period at 2-8°C. Second, 30 µl of buffer solution and 20 µl of Anti-Biotin Microbeads were added, following another incubation period of 10 minutes at 2-8°C. Meanwhile, an LS column was placed in a magnetic field of a MACS separator and rinsed with 3 ml of buffer. Cell suspension was placed into the column, subsequently the column was washed with another 3 ml of buffer. CD8+/CD4+ cells were collected in the flow through and washed once with PBS. Viability was determined using the trypan blue stain - one spleen produced a median of $2x10^7$ viable cells.

Enriched T cells were resuspended in 1ml culture media at a density of $1x10^6$ cells per tube, labeled using Cell Trace Violet (see below), stimulated with anti-CD28 (1 µl/ml) and anti-CD3e (1.8 µl/ml) mAbs and divided into treatment and non-treatment groups. Increasing concentrations of PFK-158 (0-10 µM) were directly added to the treatment group.

Leukocytes from ascites of tumor-bearing mice were isolated by discontinuous Ficoll gradient and stained for flow cytometric analysis as described below.

ACK buffer (premixed)

155 mM	NH_4CL
1 mM	$KHCO_3$
0.1 mM	EDTA
pH 7.2	

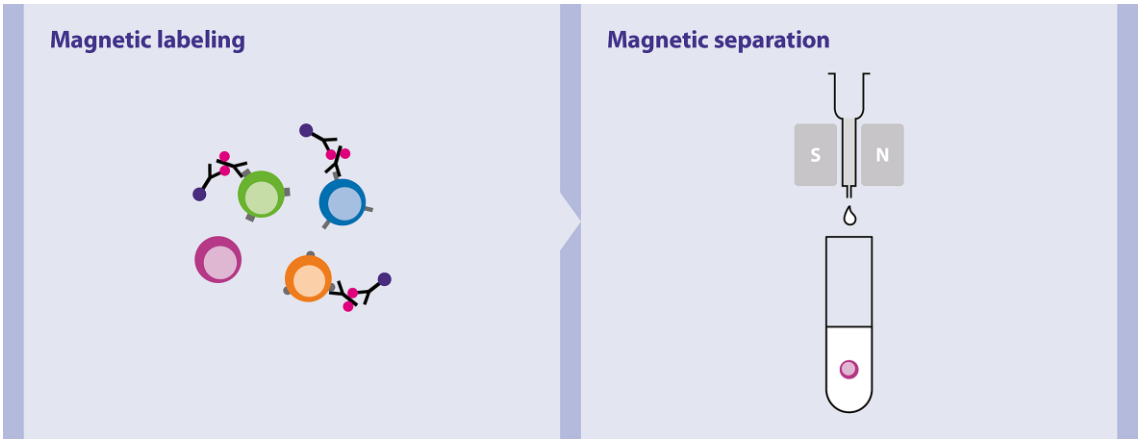

Fig. 3: Isolation of unlabeled (untouched) T cells (represented by purple cell) by magnetic separation. Non-target cells are labeled and retained within the magnetic column (LS Coulumn) while the target cell type is collected in the flow-through. Figure provided by Miltenyi Biotec.

V.2.3 Glycolytic inhibitor

PFK-158 is developed and supplied by Advanced Cancer Therapeutics, Louisville, KY, USA. For the *in vitro* and *in vivo* studies, PFK-158 was dissolved in PBS and for *ex vivo* studies, PFK-158 was dissolved in DMSO.

V.2.4 In vitro proliferation assay

The anti-proliferative effect of PFK-158 was assessed using the MTT colorimetric assay, as described by Mosmann (Mosmann, 1983).

PFK-158 was dissolved in PBS to a stock concentration of 30 µM.

M505 and STOSE cells were washed with PBS, trypsinized with 0.25 % trypsin-EDTA at 37°C and seeded in triplicates into 96-well plates at a density of 3×10^3 cells per well with 200 µl of media. Serial dilutions were prepared from the stock solution in complete culture media. After 24 hours, media was removed and the treatment regimen of PFK-158 at different concentrations was added for 24 or 48 hours.

After the required drug incubation period, 20 µg per well of 3-(4,5-dimethylthiazol-2-yl)-2,5-diphenyl tetrazolium bromide (MTT) was added to culture media and further incubated for 1-2 hours at 37 °C. Remaining media was then removed and generated formazan crystals were dissolved in 200 µl DMSO. Optical density was measured at 570 nm in a multimode plate reader (Biotek, USA).

V.2.5 Glucose uptake assay

Glucose uptake assay was performed as previously described with minor modifications for isolated T cells (Mondal et al., 2015). Two groups of M505 and STOSE cells were plated in triplicates at a density of $1x10^4$ cells per chamber in 500 µl growth media per chamber in a 4-well chamber slide and incubated for 24 hours. Following the incubation period, one group was treated with 5 µM PFK-158. Both groups were incubated for another 60 minutes and the growth media from both groups was removed. Subsequently, all cells were treated with 2-NBDG (30 µl/ml) for 30 minutes in 200 µl of glucose free RPMI-1640 media. Cells from both groups were washed in PBS and the glucose uptake of the live M505 and STOSE cells was measured and analysed in the Zeiss LSM510 fluorescence microscope (Oberkochen, Germany). Fluorescent intensities were calculated using ImageJ software.

Four groups of isolated T cells (CD4+/CD8+) were plated in triplicates at a density of $2x10^6$ cells/tube in 3 ml growth medium per tube, three groups were stimulated with anti-CD28 and anti-CD3e mAbs for 24 hours. Following the stimulation period, growth media was removed and all groups were submitted to a starvation period of 15 minutes in glucose free media (Krebs-Ringer solution, HEPES buffered). PFK-158 was added to glucose free media of two stimulated groups at 2.5 µM and 5 µM for another 60 minutes respectively. 500 µl glucose free media containing 1 µCi/ml of the fluorescent glucose tracer 2DG (Perkin Elmer, Waltham, MA, USA) was then added to all groups, and cells were incubated for a further 120 minutes. Cells were subsequently pelleted, washed in PBS and lysated in 300 µl of H_2O. Lysate was transferred in a 96-well plate and glucose uptake was measured and analysed for each condition via fluorescence using the Synergy HTX Multi-Mode Reader.

V.2.6 ATP colorimetric assay

The mitochondrial ATP production was measured using the ATP colorimetric assay kit (BioVision, Milpitas, CA, USA). M505 and STOSE cells were plated in duplicates at a density of 1.5×10^5 cells (untreated and treated with PFK-158, 0–10 µM) per well in a 6-well plate and incubated for 24 hours. Four groups of enriched T cells (CD4+/CD8+) were resuspended at a density of $2x10^6$ cells/tube in 3 ml growth medium per tube. Three groups were stimulated with anti-CD28 and anti-CD3e mAbs and rising concentrations of PFK-158 (2.5 – 5 µM) were added for 72 hours.

Then, cells were lysed in 100 µl ATP assay buffer. 50 µl of each sample was then added to a 96-well plate. The standard curve (using rising volumes of ATP standard, ddH_2O and adjusting to 50 µl/well with ATP assay buffer) was prepared, thus generating 0, 2, 4, 6, 8, 10 nmol/well of ATP standard for further reference. A reaction mix was prepared (containing 88 % ATP assay buffer, 4 % ATP probe, 4 % ATP converter and 4 % developer with specified volume mentioned in the manufacturer's protocol) and added to each well (50 µl/well) containing the ATP standard and test samples. Following an incubation period in the dark for 30 minutes at RT, absorbance was measured at 570 nm in a micro-plate reader. Mitochondrial ATP production was presented at nmol/µl by referencing the OD values of the standard curve.

V.2.7 Western blot analysis

Cell lysate

Immunoblot analysis was performed using protein lysates of STOSE and M505 cells ($8x10^4$), either treated with PFK-158 (0-15 µM) for 24 hours or untreated, as well as enriched T cells ($1.25x10^6$) treated with PFK-158 (0-5 µM) for 72 hours or untreated. Cells were collected, lysed in a cold lysis buffer (CLB, Cell Signaling Technology, Danvers, USA for STOSE and M505; MTBB lysis buffer for T cells) containing an added protease inhibitor cocktail (Roche, Indianapolis, IN, USA) and centrifuged at 13,000 rpm for 5 minutes at 4°C. Supernatant was collected.

Cell lysis buffer (premixed)

20 nM	Tris-HCl
150 nM	Sodium chloride
1 nM	NA_2EDTA
1 mM	EGTA
1 %	Triton
2.5 nM	Sodium pyrophosphate
1 mM	Beta-glycerophosphate
1 mM	Na_3VO_4
1 µg/ml	Leupeptin
pH 7.5	(Protease inhibitor added)

MTBB lysis buffer

0.2 %	Tween 20
0.2 %	NP-40
10 %	Glycerol
150 mM	Sodium chloride
25 mM	HEPES
5 mM	EDTA
0.5 mM	Calcium chloride
pH 7.4	

Determining protein concentration

Protein concentration was measured by the Bradford method (Bio-Rad, Hercules, CA, USA). The Bradford assay is a colorimetric protein assay based on the absorbance of Coomassie Brilliant Blue GL250 dye colour change in response to various concentrations of protein. The Bradford reagent was diluted in a 1:5 ratio with deionized H_2O, 500 µl of the diluted reagent were mixed with another 500 µl ddH_2O and 1 µl of protein sample was added. To determine protein concentration, absorbance was measured at 595 nm with a spectrophotometer.

SDS-polyacrylamide gel electrophoresis

Protein samples with equal protein amounts were denaturated by adding 5 µl LDS sample buffer to each sample and heated at 95°C for 2 minutes. Samples were then loaded into the wells of the SDS-PAGE gel (polyacrylamide gel electrophoresis, 4–12.5 % gradient) along with a molecular weight marker. Running buffer was added to the tank and samples were run at 70 V for approximately 2-3 hours.

Sample buffer (premixed)

988 mM	Tris
2.04 mM	EDTA
8 %	LDS
40 %	Glycerol
0.88 %	Coomassie Brilliant Blue GL250
0.7 mM	Phenol red
pH 8.4	

Running buffer (premixed)

25 mM	Tris
192 mM	Glycine
0.1 %	SDS
pH 8.3	

Transfer to the membrane

Carbon paper and nitrocellulose membrane were cut to size of the separating gel and soaked in the transfer buffer containing 60 % ddH_2O, 20 % premixed transfer buffer and 20 % ethanol. Separating gel was carefully removed from the plastic cassette and briefly soaked in transfer buffer. The transfer stack was prepared in the following order (bottom to top): sponge, carbon paper, gel, membrane, carbon paper, sponge. The electrotransfer was performed at 25V for 14 minutes using the Trans-blot transfer system by Bio-Rad.

Transfer buffer (premixed)

25 mM	Tris
192 mM	Glycine
pH 8.3	

Antibody staining

Following the electrotransfer of protein, the membrane was blocked for 60 minutes in the blocking solution (5% TBS–BSA) at RT and probed overnight with primary antibodies (1:500) at 4°C. Following incubation, the membrane was washed with 0.1 % Tween-20 containing TBS (TBS-T) and probed with fluorophore-conjugated secondary antibody (1:10,000) in blocking buffer for 60 minutes at RT. The blots were washed three times in TBST and target proteins were visualized using the LI-COR machine and analyzed using the Odyssey Imaging System (Lincoln, Nebraska, USA).

Blocking buffer

25 mM	Tris
192 mM	Glycine
0.1 %	Tween 20
5 %	BSA
pH 7.4	

V.2.8 CellTrace Violet labelling of T cells

CellTrace Violet is a fluorescent dye commonly used with flow cytometry to identify lymphocyte proliferation by labelling individual generations. Hereby, the CellTrace reagent diffuses into individual cells and binds to intracellular amines.

Enriched T cells were labelled using the Cell Trace Violet Proliferation Kit (Thermo Fisher Scientific, Waltham, MA, USA) by first diluting CTV in DMSO to the working concentration and then adding 5 µM of the dye with $1x10^6$ T cells. Aliquots were immediately vortexed to ensure rapid and homogeneous labelling of cells and incubated for 30 minutes at 37°C in the dark. Samples were quenched with culture media for 5 minutes to wash out unbound dye. Cells were then washed in PBS, stimulated and cultured at different conditions, as previously described. Analysis was performed on the 6^{th} day.

V.2.9 Flow cytometry

Cell surface and intracellular molecule staining as well as flow cytometry were performed as described by Knutson (Knutson, Almand, Dang, & Disis, 2004) by the Department of Immunology at Mayo Clinic.

Splenocytes were harvested from FVB mice by careful dissection, following T cell isolation and analysis.

T cells were washed in PBS with 1 % BSA and incubated with 5-40 µl of primary antibody added at 4°C for 30 minutes, followed by three wash cycles. Antibodies against CD4, CD8, CD25, Foxp3 (Treg), T-bet (Th1), GATA3 (Th2), RORɣt (Th17) were obtained from eBiosciences (San Diego, California, USA). Recommended isotype-matched non-specific antibodies were used as controls. For intracellular staining, cells were permeabilized before the application of antibodies using CytoFix/Cytoperm (BD Biosciences, San Diego, California, USA). T cells were then fixed in 1 % paraformaldehyde, subsets were gated on CD4/CD25 viable cells and analysed on the flow cytometer using FlowJo 10.8.1 software (Becton Dickinson, Franklin Lakes, NJ, USA).

V.2.10 Enzyme-linked immunosorbent assay (ELISA)

ELISA analysis was performed by the Department of Immunology at Mayo Clinic.

Levels of cytokine in culture media (*ex vivo*), plasma and ascites (*in vivo*) were measured in duplicates for each condition using the human IFNɣ/IL-4/IL-17/IL-10 Quantikine ELISA kit (R&D Systems, Minneapolis, MN, USA) according to the manufacturer`s instruction.

For *ex vivo* experiments, splenocytes from FVB mice were harvested by careful dissection and divided into two groups, stimulated and treated with different concentrations of PFK-158. Cytokines contained in the culture media were measured after three days of treatment (group 1) or three days of treatment followed by three days of incubation in culture media (group 2).

For *in vivo* experiments, cytokines contained in plasma and ascites were measured directly.

In brief, 96-well plates coated with mouse-specific IL-10 (or IL-17; IL-4; IFNɣ, respectively) were filled with 100 µl of 1:1 diluted standard, control or treated sample and incubated for 2 hours at RT. After four washing cycles, 100 µl of polyclonal antibody specific for mouse IL-10 (or IL-17; IL-4; IFNɣ, respectively) were added and incubated for another 2 hours at RT. After washing, 100 µl of tetramethylbenzidine were added and incubated for 30 minutes on the benchtop, while protected from light. Colour development was stopped by the addition of 100 µL/well of diluted hydrochloric acid and absorbance was read at 450 nm on a microplate reader.

V.2.11 Syngeneic mouse model

A syngeneic ovarian cancer model was established by intraperitoneal injection of STOSE cells (1.5×10^7 in a total volume of 200 µl in PBS) into the right lower abdomen of female 8-week-old mice (FVB strain, Jackson Laboratory). This was considered day 0. On day 35 after injection, mice were randomized into two groups ($n_1=8$; $n_2=8$) and treatment of group 2 was initiated (PFK-158 at 60 mg/kg via i.p.-injection every 48 hours for 20 days).

Disease progression, weight and abdominal girth were monitored throughout the complete duration of the experiment and efficacy of treatment was assessed by comparing tumor and ascites volumes between the treatment and control groups at

the time of autopsy at day 55. Blood samples were obtained from the facial vein of all animals by cheek bleeds (approximately 200 µl per mouse), centrifuged and stored at -80°C. Ascitic fluid was aspirated through a needle inserted into the mouse`s peritoneal cavity after euthanasia and centrifuged. The supernatants were stored at -80°C while the cell pellets were frosen in DMSO following red cell lysis. Spleens were removed and placed on ice in cold PBS. Tumor deposits were fixed in 10% neutral buffered formalin (Thermo Fisher Scientific, Rockford, IL, USA), embedded in paraffin, sectioned at 5 µm and stained for histologic analysis.

V.2.12 Immunohistochemistry

Formalin-fixed tumor tissue samples were embedded in paraffin and sectioned at 5 µm for histologic analysis. Cell proliferation was evaluated by staining for anti-Ki-67 and tumor-infiltrating CD8+ T cells were quantified both in the tumors of the control and treatment groups by staining for murine anti-CD8+. Immunohistochemistry was performed by the Pathology Research core facility at Mayo Clinic. CD8+ cells were counted in 5 HPF of viable tumor tissue per mouse, the numbers were averaged and compared between the groups.

V.2.13 Statistical analysis

All results are depicted as mean ± standard deviation (S.D.). Unless mentioned otherwise data was obtained from three independent experiments. All statistical analyses were performed using the GraphPad Prism 7.05 software (San Diego, CA, USA). Data sets were analysed using unpaired t-test. The significance level was set at 0.05 ($p < 0.05$) unless determined otherwise and denoted as * (< 0.005 as **; < 0.0005 as ***; < 0.00005 as ****).

VI. Results

VI.1 In vitro

VI.1.1 PFK-158 treatment inhibits M505 and STOSE cell proliferation in a dose-dependent manner.

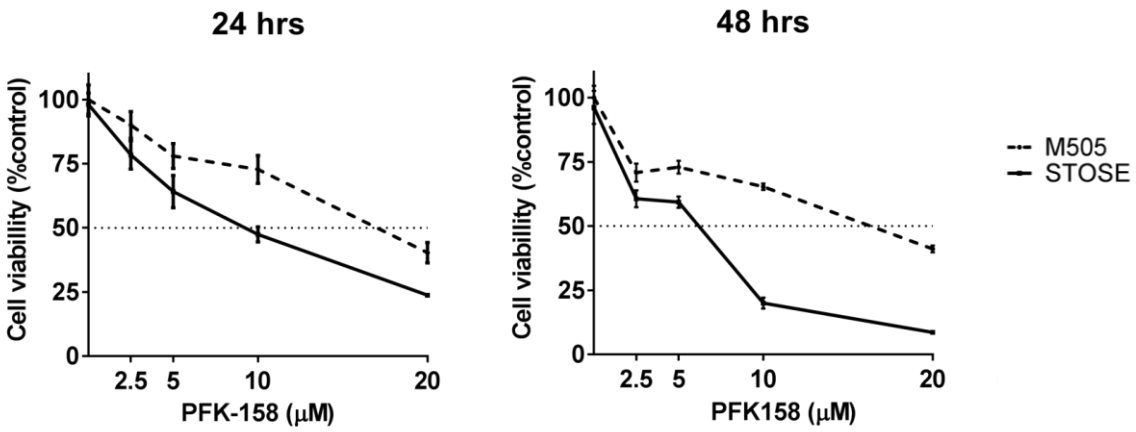

Fig. 4: Percentage of cellular viability of ovarian surface epithelial cell line (M505) and ovarian cancer cell line (STOSE) treated with increasing concentrations of PFK-158 for 24 and 48 hrs.

First, the inhibitory effect of PFK-158, a selective inhibitor of PFKFB3, on cell proliferation was investigated *in vitro*. The non-malignant control cells (M505) and ovarian cancer cells (STOSE) were exposed to a range of PFK-158 concentrations (0-20 μM) for 24-48 hours. Cell viability was assessed using the colorimetric MTT assay, which measures metabolic activity of viable cells by quantifying the transformation of the yellow tetrazolium salt 3-(4,5-dimethylthiazol-2-yl)-2,5-diphenyltetrazolium bromide into indissoluble purple formazan crystals.

The inhibition of cell viability under PFK-158 treatment is presented as the percentage of viable treated cells compared to untreated control, as shown in Figure 4. PFK-158 suppressed cell viability in a dose- and time-dependent manner in both cell lines. Non-malignant cell viability, as represented by M505 cells, was less affected by PFK-158 treatment compared to cancerous STOSE cells at both time points. Longer exposure to PFK-158 led to a decreased STOSE cell proliferation at lower concentrations of PFK-158. The IC_{50} values ranged from 16.6 μM for M505 (for both 24/48 hrs) and 6.3 μM (48 hrs) to 9.1 μM (24 hrs) for STOSE cells, respectively.

VI.1.2 PFK-158 inhibits PFKFB3 in M505 and STOSE cells in a dose-dependent manner.

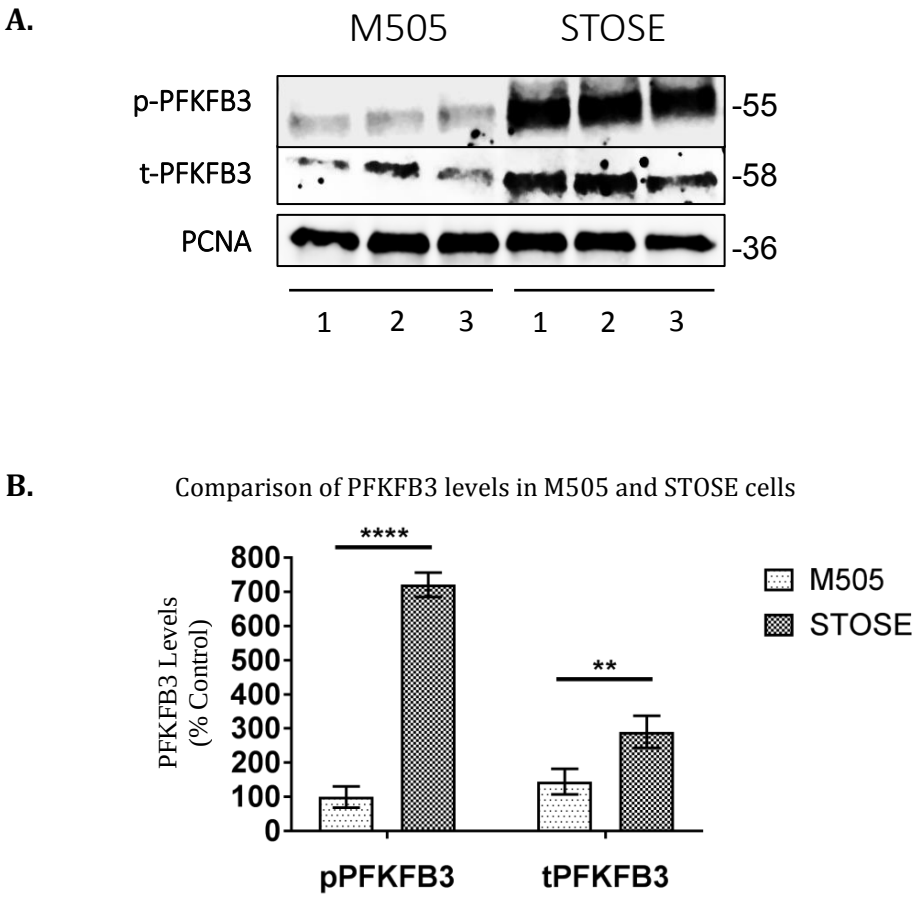

Fig. 5: Expression of p-PFKFB3 and t-PFKFB3 in ovarian surface epithelial cell line (M505) and ovarian cancer cell line (STOSE). PCNA was used as the loading control. Data are shown as mean ± SD for three replicates per cell line (A.). Band intensities were quantified and are presented as bar graphs (B), ***P* < 0.005; *****P* <0.00005.

Second, we investigated whether decreased cell viability under PFK-158 treatment was linked to inhibition of PFKFB3, as elevated levels of activated PFKFB3 have been previously demonstrated in ovarian cancer and malignant pleural mesothelioma (Mondal et al., 2019; Sarkar Bhattacharya et al., 2019).

First, the expression levels of total- and phospho-PFKFB3 (activated form) were determined in both malignant and non-malignant cell lines. Immunoblot analysis showed significantly higher levels of t-PFKFB3 and p-PFKFB3 in OC cells, as presented in Fig. 5. An approximate seven-fold increase of the activated phospho-

PFKFB3 was measured in STOSE cells, further supporting the argument of a higher glycolytic rate in malignant cells.

Subsequently, both cell lines were incubated with increasing concentrations of PFK-158 (0-15 µM) for 24 hours, which showed a dose-dependent inhibition of t-PFKFB3 and p-PFKFB3 by immunoblot analysis in M505 and STOSE cells (Fig 6).

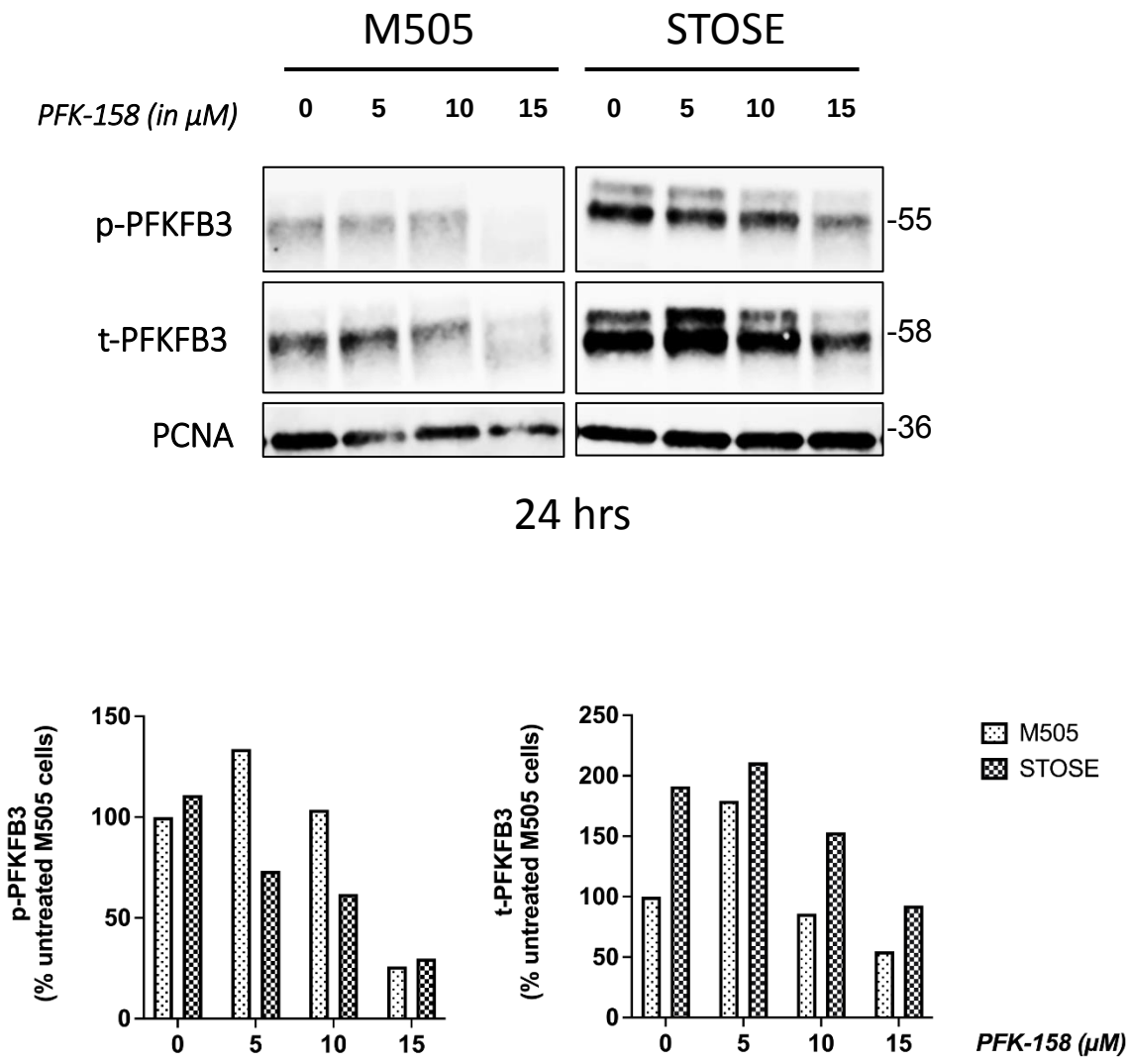

Fig. 6: Decreasing levels of t-PFKFB3 and p-PFKFB3 with 24 hours PFK-158 treatment in M505 and STOSE cells. PCNA was used as the loading control.

VI.1.3 Inhibition of PFKFB3 with PFK-158 reduces glucose uptake and intracellular ATP production in OC cells.

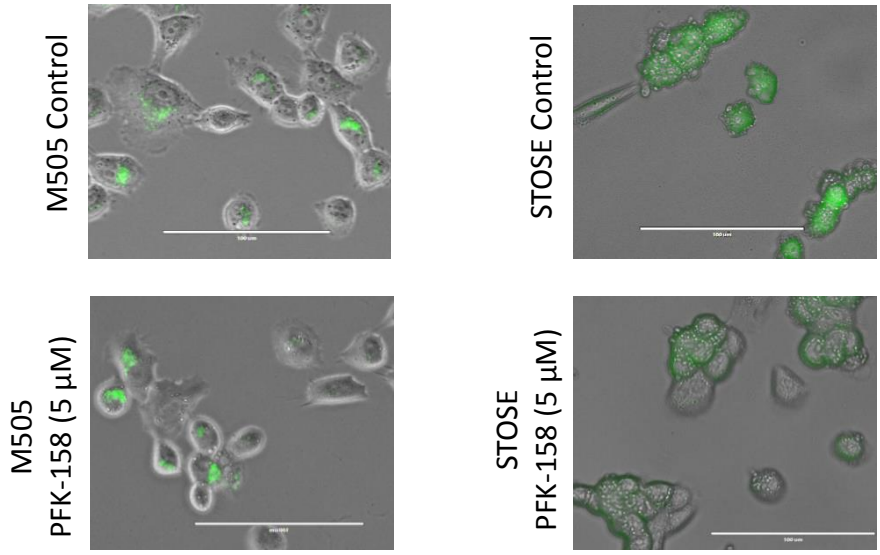

Fig. 7: Fluorescence images of glucose uptake (green) using 2-NBDG in M505 and STOSE cells. Scale bar: 100 µm. Glucose uptake is inhibited by PFK-158 treatment in STOSE cells.

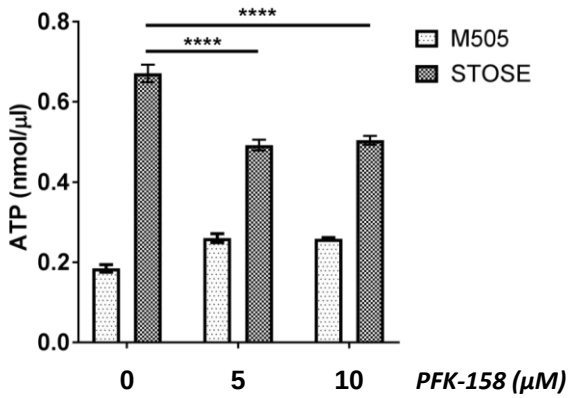

Fig. 8: Intracellular ATP generation in M505 and STOSE cells in the presence and absence of PFK-158.

Finally, in order to evaluate, whether treatment with PFK-158 also reduces the glycolytic rate, glucose uptake and intracellular ATP levels in M505 and STOSE cells were determined in presence and absence of different concentrations of PFK-158. Results revealed a decrease in glucose uptake in STOSE cells after treatment with PFK-158 for 24 hours, as determined using 2-NBDG, a fluorescent glucose analog. M505 cells showed an overall lower glycose uptake in comparison to their malignant counterparts and no change under PFK-158 treatment (Fig. 7). Consistent with the decrease in glucose uptake, PFK-158 led to a reduction in intracellular ATP levels in STOSE cells and a slight increase in M505 cells (Fig. 8).

VI.2. Ex vivo

As previously described, the main focus of experimental immunological research was directed at T cell mediated response to PFKFB3 inhibition. We investigated the ability of CD8+/CD4+ cells to differentiate, proliferate and secrete cytokines in the presence and absence of PFK-158.

VI.2.1 PFKFB3 inhibitor PFK-158 decreases T-cell viability and suppresses T cell proliferation after stimmulation in a dose-dependent manner.

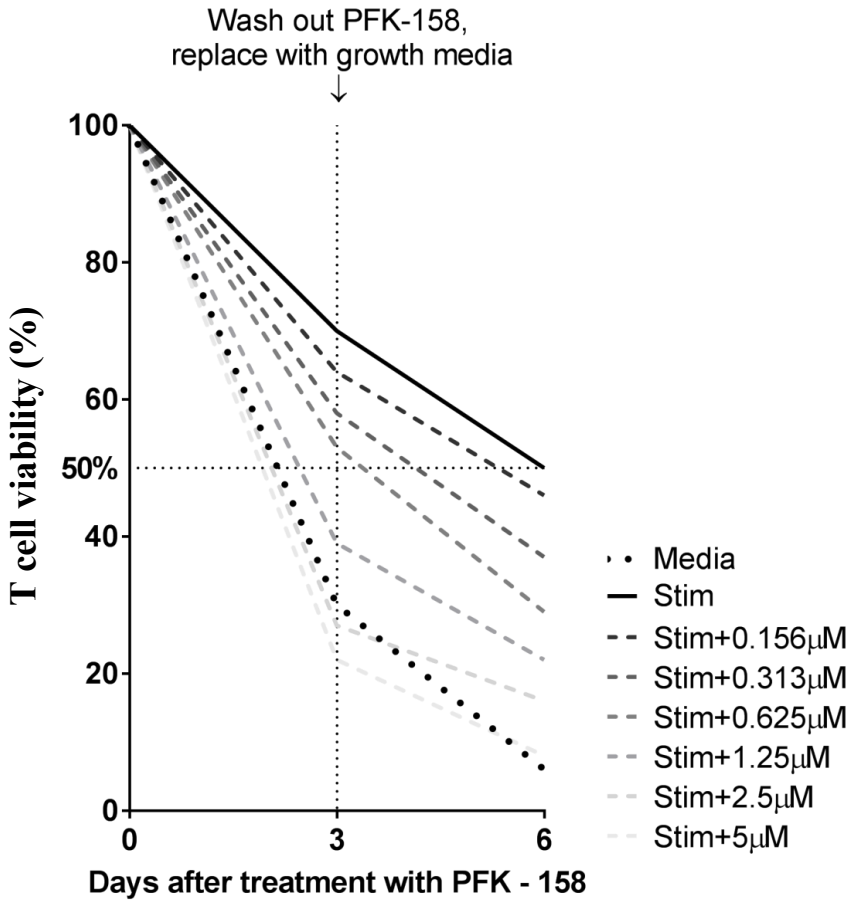

Fig. 9: Percentage of viable T cells at varying experimental conditions: untreated and unstimulated (= Media), untreated and stimulated (= Stim) and stimulated and treated with increasing concentrations of PFK-158 (0.156 - 5 μM) after three "treatment" followed by three "resting" days.

In our first *ex vivo* experiment, we established the general influence of PFKFB3 inhibition on T cell viability. Enriched T cells were equally divided into eight groups ($1x10^6$ cells per tube) and exposed to varying conditions.

The first group was left unstimulated and untreated throughout the duration of the entire experiment. The second group was cultured in the presence of microbeads precoated with the antibodies to the T cell receptor, CD3e, and the co-stimulatory surface ligand CD28. This combination closely mimics the signals of antigen presenting cells in *in vivo* conditions, initiating T cell activation upon binding. The activation occurs swiftly and does not require a prolonged time period. Groups 3-8 were stimulated in the same manner and additionally treated with increasing concentrations of PFK-158 (0.156 – 5 μM). All groups were incubated for 72 hours at 37°C, followed by washing out previous conditions and inducing a "resting" period in culture media for another 72 hours. Viable cells were counted on the 3rd and 6th day of the experiment.

As presented in Figure 9, T cell viability rapidly declined in the unstimulated and untreated condition throughout the entire duration of the experiment. Interestingly, after washing out PFK-158 and the stimulant and replacing them with culture media, previously stimulated and untreated cell viability declined at a slightly higher rate compared to previously stimulated and treated cells, which maintained a higher viability for the second half of the experiment. The highest viability overall could be observed in the stimulated but untreated group at both time points. Stimulated and treated with a lower dose of PFK-158 (up to 1.25 μM) T cells have been comparatively more vital to those treated at a concentration higher than 1.25 μM. Generally, washing out PFK-158 resulted in higher viability throughout days 4-6, whereby cell death in the second half of the experiment was lowest in the stimulated and treated with 2.5 μM PFK-158 condition.

To further investigate the possible effects of PFK-158 on T cell proliferation, fluorescent labeling of cells by CellTrace violet was performed. This dye permanently labels cells by engaging in covalent bonding to intracellular amines without affecting morphology or physiological properties of the cells. Through subsequent cell divisions, daughter cells receive about ½ of the parental fluorescent label, which allows for generational tracing by analyzing fluorescence intensity levels using flow cytometry.

The unstimulated parent generation (M1) is represented inside the red square, while peaks in the blue square (M2-M7) represent successive generations of live CD4+ T cells.

Enriched unstimulated and untreated CD4+ T cells (resuspended in culture media) remained in a quiescent state. In contrast, activated by anti-CD28 and anti-CD3e CD4+ T cells exhibited rapid proliferation, which could be followed up to the 6^{th} generation (M2-M7).

In comparison, the percentage of proliferating CD4+ T cells was visibly reduced at 1.25 μM PFK-158. However, no generational tracing is detectable at 2.5 and 5 μM PFK-158, indicating a dose-dependent suppression of CD4+ T cell proliferation and finally its impairment at a concentration of 2.5 μM PFK-158.

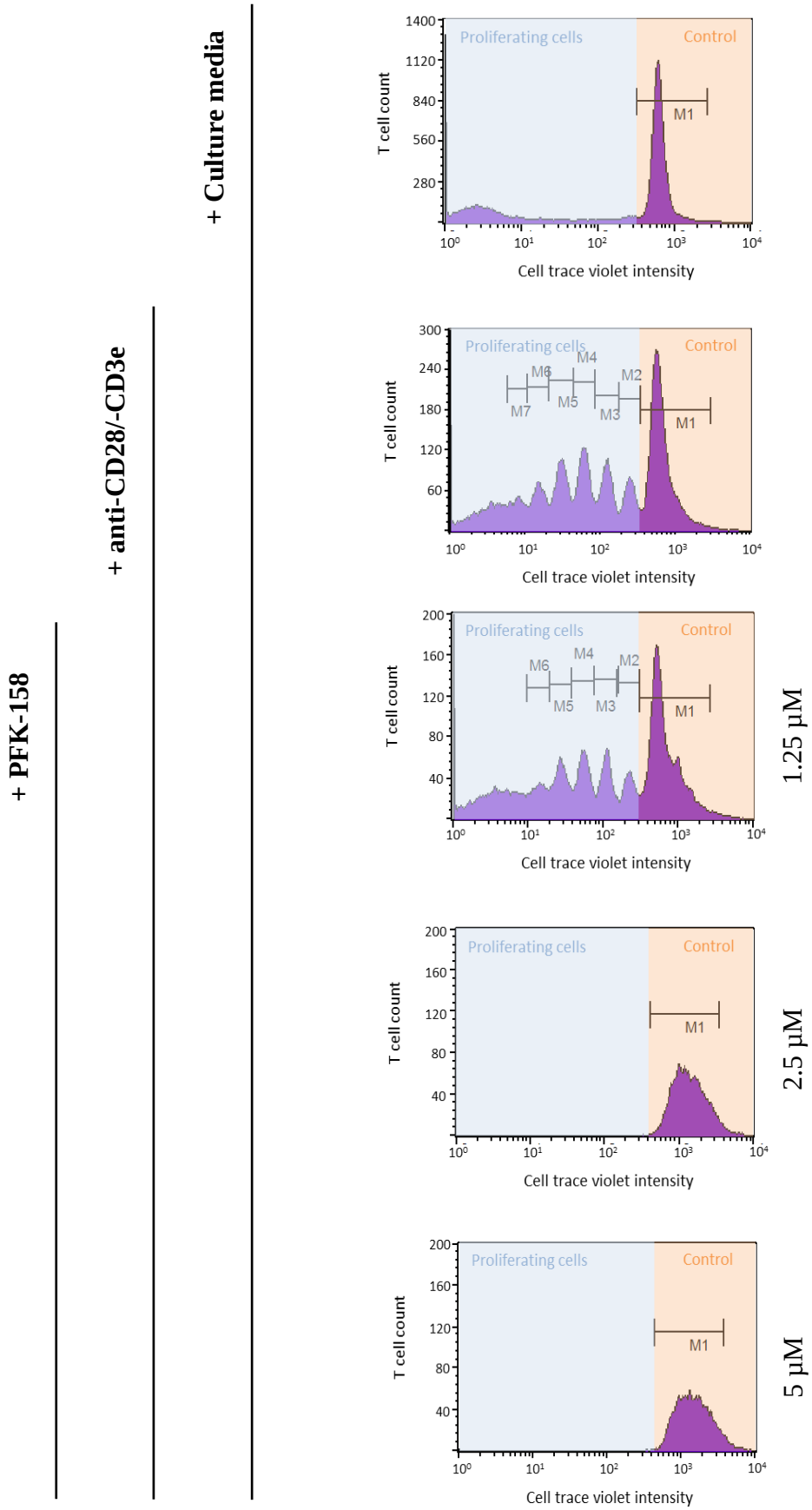

Fig. 10: Histogram plots of CellTrace intensity gated on CD4+ T cells illustrating T cell proliferation *ex vivo* under varying conditions (represented by subsequent generations M2-M6) after three "treatment" followed by three "resting" days. The analysis was performed on day 6.

VI.2.2 The small molecule antagonist PFK-158 reduces anti-CD3e/anti-CD28-induced PFKFB3, glucose uptake and intracellular ATP production of T cells.

The effect of PFK-158 treatment on expression levels of PFKFB3 in CD4+/CD8+ T cells was investigated in the same manner as previously in M505 and STOSE cells. Stimulation of T cells by anti-CD28 and anti-CD3e antibodies led to a substantial increase of both p-PFKFB3 and t-PFKFB3 levels, which were in turn suppressed by PFK-158. The highest suppression level of activated PFKFB3 was observed at 1.25 µM of the glycolytic inhibitor. However, p-PFKFB3 levels showed an opposite response to increasing concentrations of PFK-158 – at 5 µM, p-PFKFB3 expression levels are similarly high to those of stimulated and untreated T cells.
The t-PFKFB3 levels were continuously reduced by PFK-158 treatment in activated T cells.

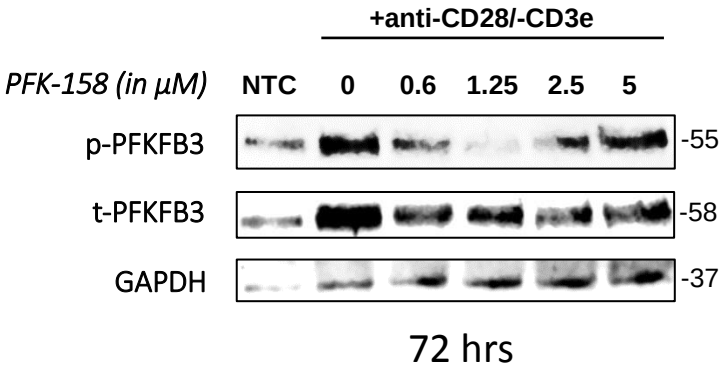

Fig. 11: Expression levels of p-PFKFB3 and t-PFKFB3 with PFK-158 treatment for 72 hours in quiescent (= NTC) and activated T cells. GAPDH was used as the loading control.

As previously described, activated T cells primarily utilize glucose to meet higher energy demands in contrast to their naïve counterparts. To investigate the effect of PFKFB3 inhibition on the metabolic state, we assessed T cell glucose uptake in the presence and absence of stimulation by anti-CD28 and anti-CD3e antibodies und added PFK-158.
Stimulated T cells expressed an approximate 3.5-fold increase in glucose uptake compared to the quiescent control, while the addition of 2.5 µM and 5 µM PFK-158 led to its significant reduction, as measured by fluorescence of the glucose tracer 2DG (Fig. 12). A dose-dependent manner of the glucose uptake reduction was not observed. Glucose uptake levels in T cells treated with PFK-158 up to 5 µM remained higher than those of the control.

These data support the conclusion that PFK-158 inhibits anti-CD3e/anti-CD28-induced PFKFB3 synthesis which in turn results in reduced glucose uptake and subsequently, a decreased intracellular ATP concentration. Despite the lack of a statistically significant result, a clear trend towards reduced ATP generation with growing PFK-158 concentration can be observed. A rapid ATP decrease, as presented in comparison with STOSE cells, does not occur.

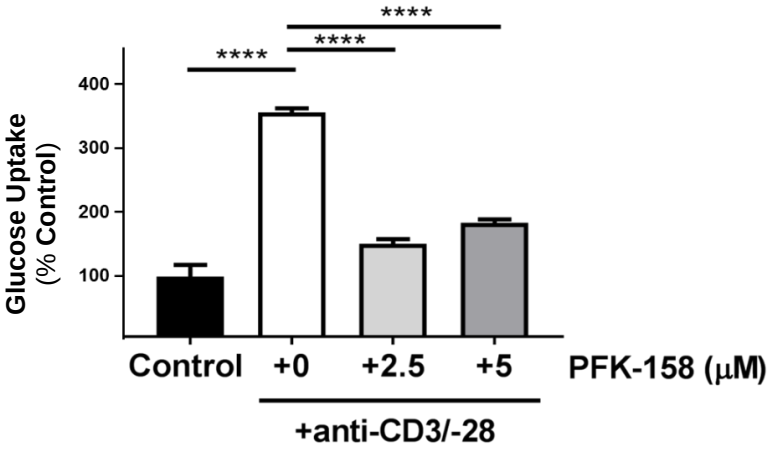

Fig. 12: CD4+ and CD8+ T cell glucose uptake was assessed using 2DG and presented as percentage of control in presence and absence of stimulation and PFK-158 (n=3; ****P <0.00005)

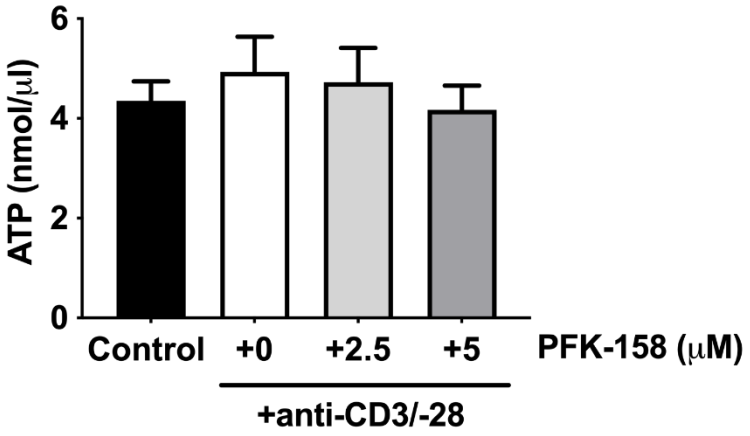

Fig. 13: Intracellular concentrations of ATP in CD4+ and CD8+ T cells in presence and absence of stimulation and PFK-158 (n=3).

VI.2.3 Quantitative analysis of PFKFB3 inhibition on T cell function.

In order to assess, whether the reduction of PFKFB3 as well as glucose uptake and ATP concentration caused by PFK-158 may be sufficient to disrupt T cell function, an analysis of inflammatory mediators secreted by various T cell subsets was performed. Cytokines can not only affect T cell proliferation but also influence cell survival, which makes them a relevant factor in the anti-tumor immune response. The emphasis was put on metabolites secreted by T cells and known to directly or indirectly impact the disease outcome.
Signature cytokines of different T cell subsets and their role in cancer progression are listed in Table 1.

Table 1: Signature cytokines of various T cell subsets and their role in EOC.

Metabolite	Origin	Evidence in cancer
IL-4	Th2	Mediates cancer cells` apoptotic resistance *[1]
IL-10	Treg	Higher serum levels in advanced cancer stages *[2]
IL-17	Th17	High levels believed to correlate with tumor progression *[3]
IFN-ɣ	Th1/CTL	Low levels found to be associated with EOC *[4]

*[1] (Kioi et al., 2005; Todaro et al., 2008)
*[2] (Rabinovich, Medina, Piura, & Huleihel, 2010; L. Zhang, Liu, Wang, Wang, & Sun, 2019)
*[3] (Yao et al., 2014; X. Zhang et al., 2014)
*[4] (Block et al., 2015; Gao, Hu, & Zhu, 2022; Wall, Burke, Barton, Smyth, & Balkwill, 2003)

To investigate the effect of PFKFB3 inhibition on T cell function, groups of equal enriched T cell amounts were stimulated by anti-CD28/CD3e and treated with rising concentrations of PFK-158 for 72 hours. The control group was composed of unstimulated and untreated T cells in culture media. In order to research, whether exposure to PFK-158 had an irreversible effect on T cell function, a second group subsequently underwent a 72 hour rehabilitation phase in culture media.
Cytokine production was higher in activated T cells, with IL-10 showing the highest absolute levels of cytokine concentration, followed by IL-4, IL-17 and finally IFN-ɣ. PFK-158 inhibited the production of IFN-ɣ, IL-4, IL-10 and IL-17 in a dose-

dependent manner, as shown in Figure 13. However, it is important to note the difference in influence of glycolytic inhibition between the assessed metabolites – for example, IL-4 and IL-17 were secreted even at high doses of PFK-158, whereas IFN-ɣ and IL-10 concentrations were undetectable.

Following a rehabilitation phase of 72 hours, PFK-158 showed similar inhibitory effect on cytokine production, mostly exhibiting a dose-dependent decrease. IL-10 concentration levels secreted by stimulated and treated T cells were higher after rehabilitation compared to the treatment stage, whereas IFN-ɣ, IL-4 and IL-17 concentrations showed an overall decline.

To properly visualize the rehabilitative properties of T cells, cytokine production after 3 and 6 days was depicted normalized to the number of viable cells (Fig. 14, right column). After PFK-158 was washed out and replaced by fresh stimulant and culture media, production levels relative to cell number increased for all assessed cytokines, indicating a reversible effect of temporary glycolytic inhibition. IFN-ɣ and IL-10 showed comparably low concentration levels at 5 μM PFK-158 at both time points, while lower dosage of the inhibitor has led to higher cytokine secretion per cell after the rehabilitation phase. On the contrary, IL-4 and IL-17 concentration levels at 5 μM PFK-158 notably increased after rehabilitation.

It should be pointed out, that interpretation of *ex vivo* data in relation to *in vivo* results must be viewed under a critical lens, as complex immune interactions cannot be reproduced as closely as in an *in vivo* setting. Not only does the adaptive immune system play a role in soliciting an anti-tumor response - the innate immunity, as well as the influence of cytokines secreted by cancerous cells themselves and the phenomenon of immune escape must be taken into account.

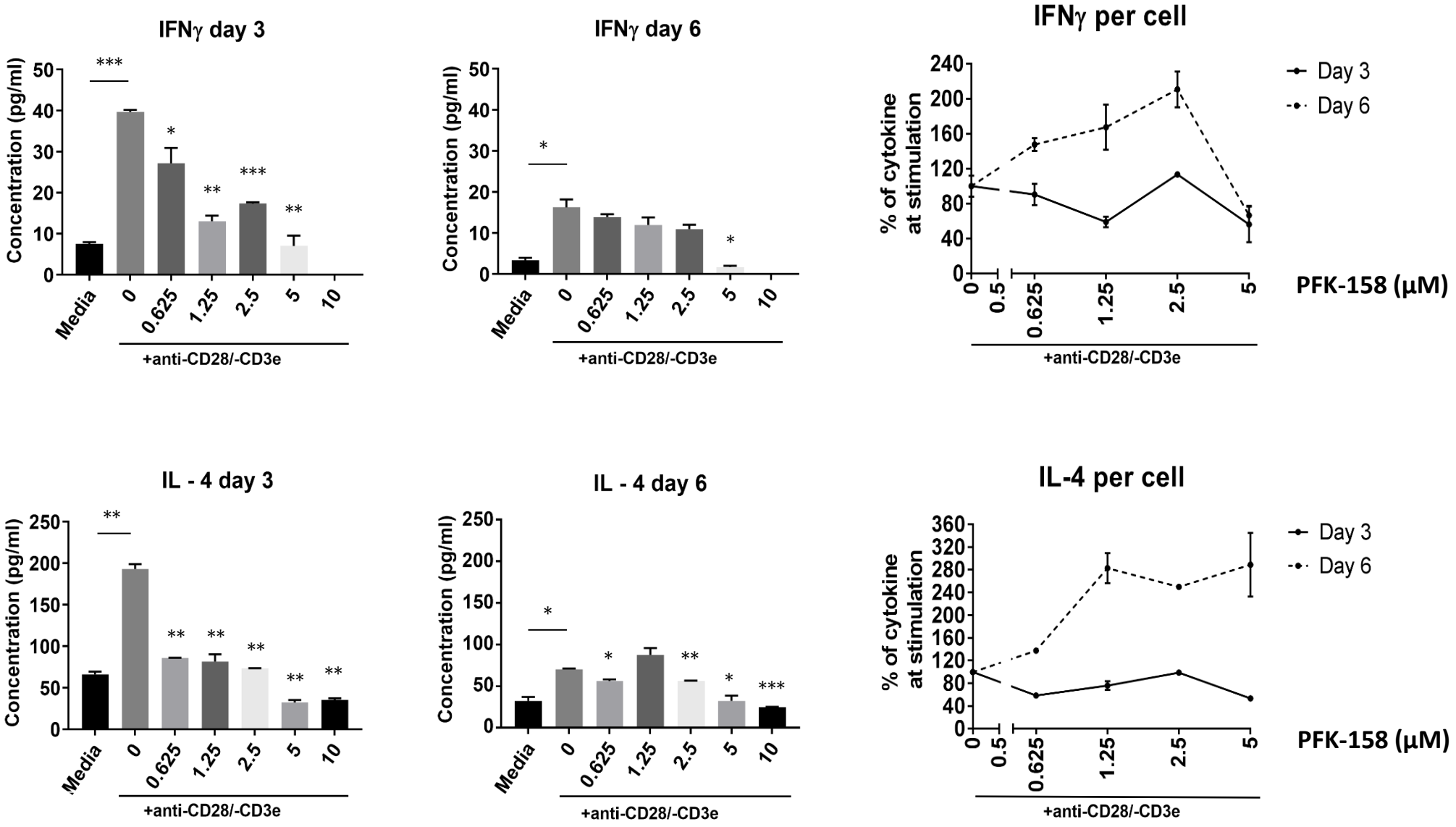

Fig 14: Cytokine production of quiescent and activated T cells under 72 hours of increasing PFK-158 concentrations and subsequent 72 hour rehabilitation phase. Left and middle: absolute IFN-ɣ and IL-4 concentration after 3 and 6 days; right: IFN-ɣ and IL-4 production as percentage of control (= stimulated, 0 µM PFK-158) normalized to viable T cells.

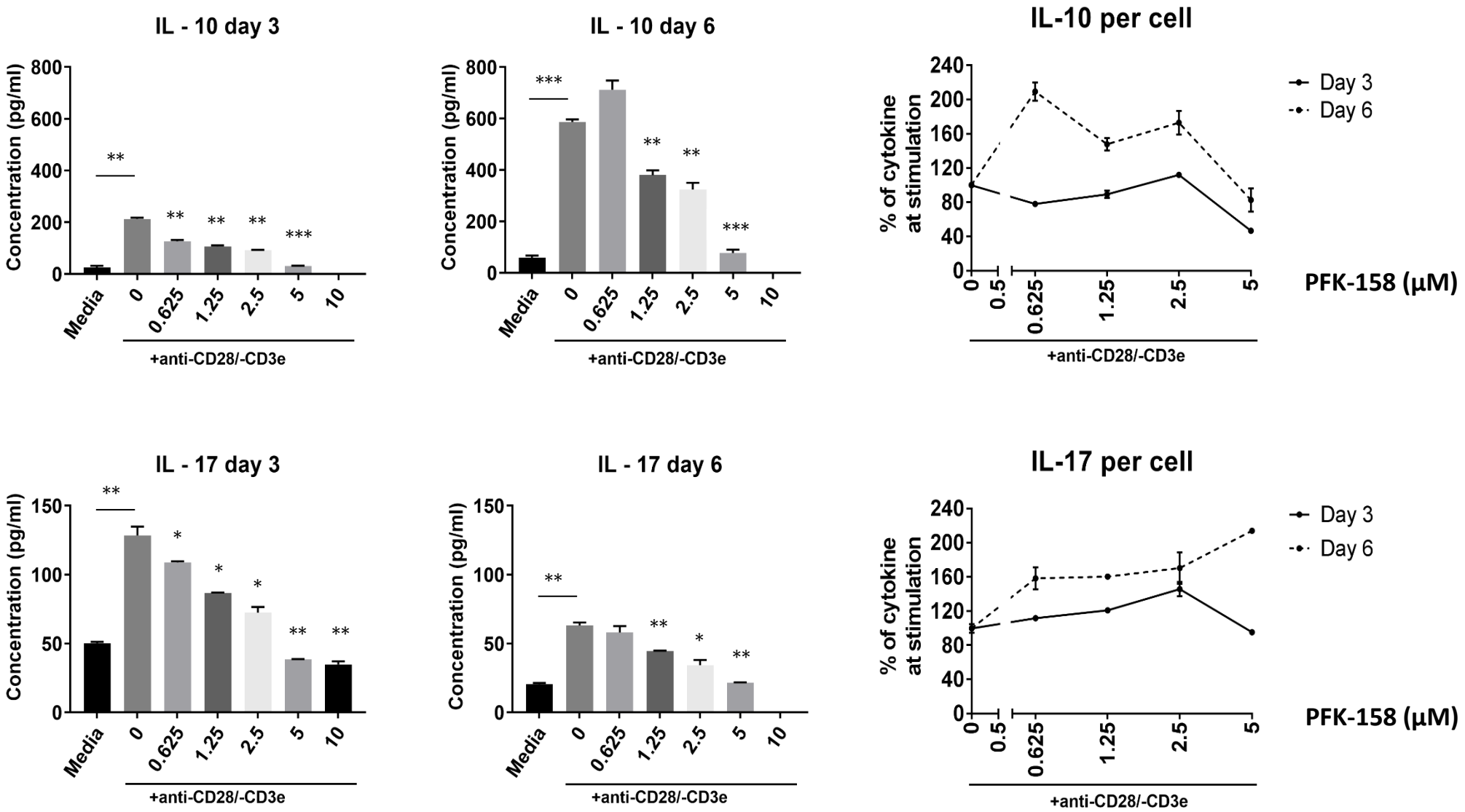

Fig 14: Cytokine production of quiescent and activated T cells under 72 hours of increasing PFK-158 concentrations and a subsequent 72 hour rehabilitation phase. Left and middle: absolute IL-10 and IL-17 concentration after 3 and 6 days; right: IL-10 and IL-17 production as percentage of control (=stimulated, 0 µM PFK-158) normalized to viable T cells.

VI.3 In vivo

VI.3.1 PFK-158 is a potent suppressor of in vivo OC tumor growth.

To further investigate whether the *in vitro* and *ex vivo* finding could be translated to an *in vivo* setting, a syngeneic mouse model was designed.

$1.5x10^7$ STOSE cells, which resemble high grade serous ovarian cancer, were intraperitoneally injected into 6 weeks old immune competent female FVB mice. Following a tumorigenesis period of 35 days, mice were subsequently either injected with PFK-158 or did not receive any treatment for 20 days, after which both groups were sacrificed and examined. To assess how well PFK-158 treatment was tolerated, the body weight and circumference of both groups was monitored (Fig.14). No weight loss was observed in the treatment group. Overall, there was no significant difference in body weight or circumference between the control and treatment group.

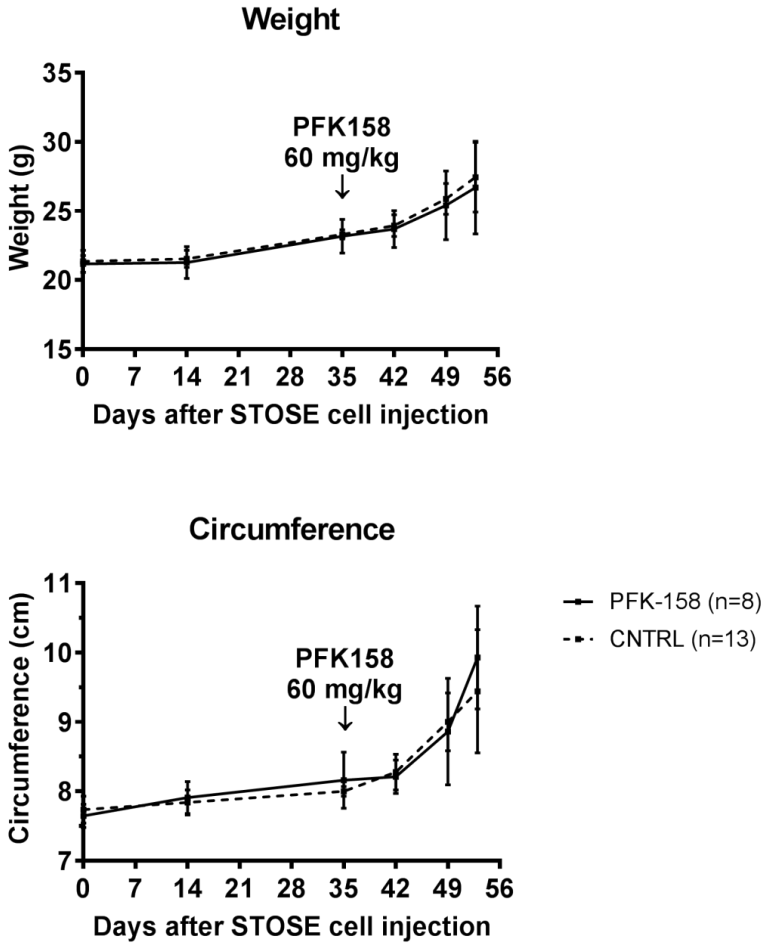

Fig 15: Changes in mouse body weight (in g) and circumference (in cm) during the experiment.

To examine the efficacy of PFK-158 and its influence on tumorigenesis of syngeneic tumors, all mice were autopsied at time of death, ascites was collected and the tumor was excised. The number of tumor bearing mice as well as mean tumor weight and ascites volume are presented in Table 2.

Table 2: Effect of PFK-158 in an in vivo mouse model; the tumor weight in the treatment group is significantly smaller compared to the control group (*$p = 0.02$).

Treatment	Mice with tumor	Tumor weight (g), mean of excised tumor	Mice with ascites	Ascites volume (ml), mean
Control	8/8	1.033	8/8	4.013
PFK-158	5/8	0.335 *	6/8	2.338

A significant reduction of tumor volume and weight was observed in the PFK-158 group. One mouse didn't show any signs of tumor development, two out of eight mice did not develop a solid intraperitoneal tumor mass, but presented small, disseminated metastatic lesions visible on the liver, peritoneum, mesentery and stomach. One mouse had to be sacrificed five days early due to an overall worsening of condition. Of the five tumor bearing mice in the treatment group, all measured tumor volumes were below 1 g, while three out of eight mice in the control group developed solid tumors over 1.2 g. These findings indicate an anti-tumor efficacy of the glycolytic inhibitor as a single agent *in vivo.*

There was no significant difference in ascites volumes between treated and untreated mice. Generally, ascites volume levels were spread over a wider range in both groups (SD Control ± 2.024; SD PFK-158 ± 2.364). While tumor mass loosely correlated with ascites volume in the control group, no such correlation was observed in the treatment group, i.e. mice with relatively small tumor mass partially presented ascites levels > 5 ml. While ascites was evenly distributed in the intraperitoneal cavity of the control group, it was mostly allocated to the left flank (injection site) in the treated mice.

Interestingly, mice in the treatment group presented a noticeably distended small intestine and colon. Microscopically, large mucinous deposits in the mesentery as well as serosal mesenteritis were detected in the histopathologic evaluation (included in supplementary data).

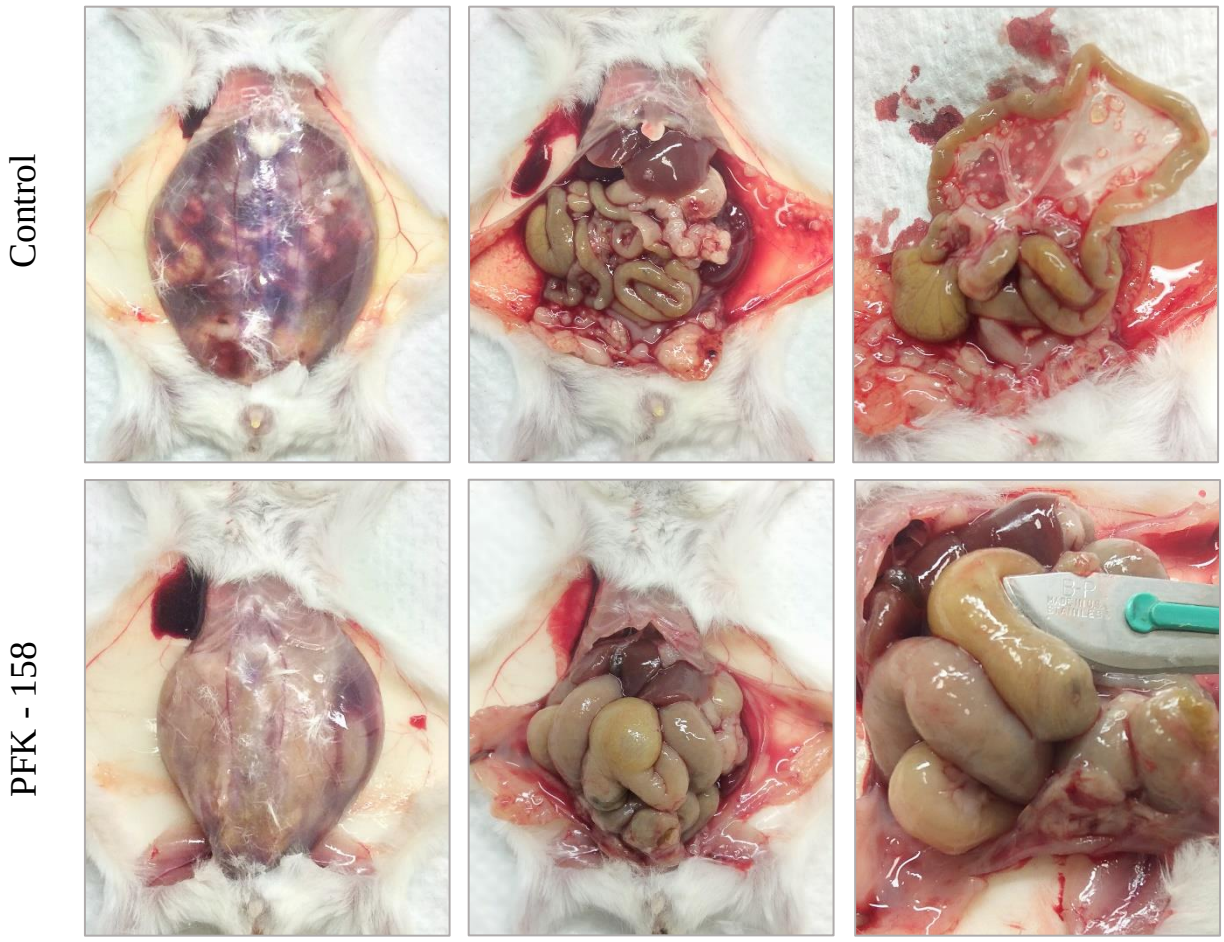

Fig. 16: Autopsy of one representative mouse per group. Left: ascitic fluid; middle: intraabdominal tumor dissemination; right: detailed depiction of metastatic nodules/bowel enlargement.

Following autopsy, paraffin-embedded tumor tissues were stained with anti-Ki67 antibody, an established cellular marker for proliferation of tumor cells. Ki67 expression was significantly downregulated upon PFK-158 treatment compared to the control group (Fig.16).

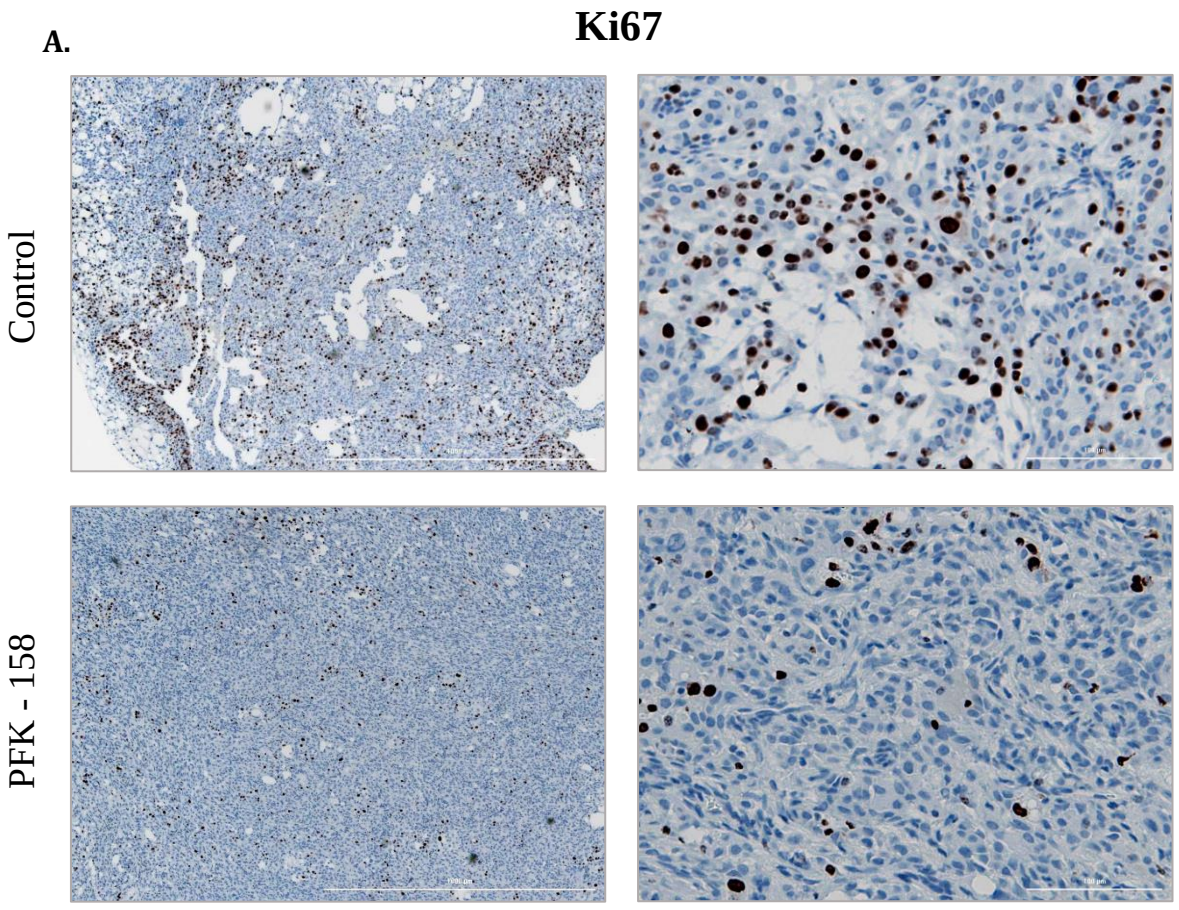

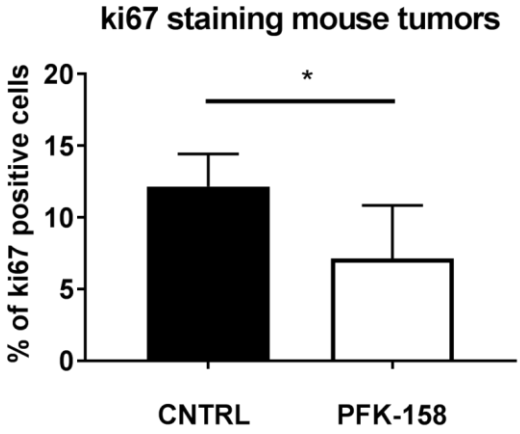

Fig. 17: IHC analysis for the expression of Ki67 in the tumors from vehicle or treated mice (A). Scale bar: 1000 µm (left); 100 µm (right). Quantitative analysis of Ki67 staining in mouse syngeneic tumor tissues across control and treatment groups. Each bar represents the mean ± SD of five independent samples per group, $*p < 0.05$ (B).

VI.3.2 PFK-158 treatment reduces IL-4 and IL-6 plasma levels in immunocompetent mice.

In order to evaluate the effect of PFKFB3 inhibition on the immune response, blood samples were collected from each mouse at day 35 immediately before beginning PFK-158 treatment and at the end of the experiment followed by autopsy on day 55. A sample size of 200 µl per mouse was chosen in accordance with the Institutional Animal Care and Use Committee (IACUC) guidelines. Plasma cytokine levels associated with EOC and possessing prognostic and clinical value (IFNɣ, IL-1β, IL-4, IL-5, IL-6, IL-10, IL-17, IL-12p70 and TNFα) were analysed via ELISA and compared between the groups. Flow cytometry could not be performed due to small sample volumes.

While there was no notable changes in the cytokine levels of IFNɣ, IL-1β, IL-5, IL-10, IL-17, IL-12p70 and TNFα, PFK-158 treatment significantly reduced the pro-metastatic IL-4 and pro-inflammatory IL-6 plasma levels compared to untreated animals.

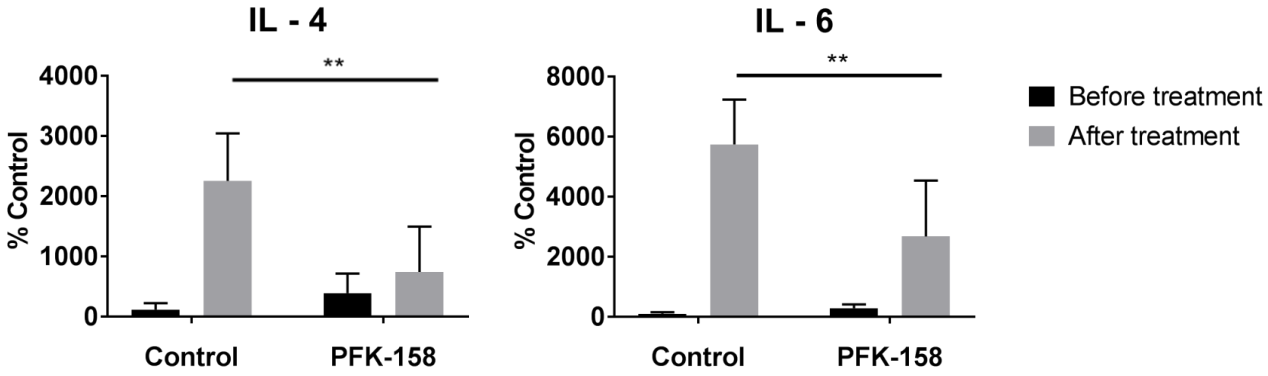

Fig. 18: IL-4 and IL-6 blood levels of both groups as percentage of control (= untreated mice at day 35 before beginning PFK-158 treatment). Each bar represents the mean ± SD of duplicates for each individual blood sample per mouse per group, ** $p < 0.005$.

VI.3.3 PFKFB3 inhibition induces the Th17/Treg ratio switch in mouse spleens.

The spleen, a secondary lymphoid organ and key site for T cell differentiation and B cell activation, plays a central role in initiating an effective anti-tumor immune response. Thus, we investigated the composition of T cell subsets in spleens of treated and untreated mice in order to assess any possible changes initiated by systemic PFKFB3 inhibition.

T cells were isolated from splenocytes as previously described and quantified via flow cytometry according to subset (Th1, Th2, Treg, Th17, CD4+, CD8+).

Interestingly, we observed a reduction of Th17 cells in the treatment group, while the amount of Treg cells simultaneously increased, indicating a reciprocal regulation of Th17 and Treg differentiation. The absolute number of CD4+ and CD8+ T cells remained comparatively similar in both groups and there was no notable difference in the Th1 or Th2 subset ratio.

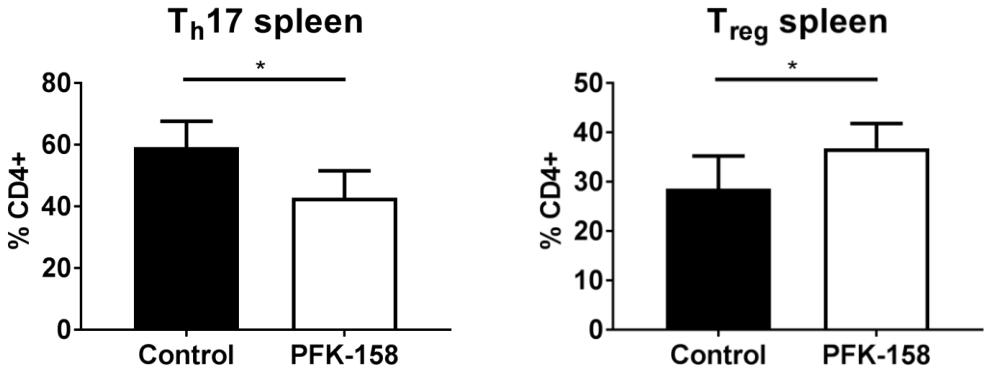

Fig. 19: Th17 and Treg levels as percentage of CD4 positive T cells in spleens of treated and untreated mice. Each bar represents the mean ± SD of single T cell counts from individual spleens according to different groups, * $p < 0.05$.

VI.3.4 Glycolytic inhibition affects the composition of the tumor microenvironment in the syngeneic OC model.

Ovarian cancer associated, malignant ascites constitutes a big portion of the extracellular matrix that forms the tumor microenvironment (TME), providing a structure for the accumulation of cellular and acellular components. It contains numerous immune cells and secreted inflammatory cytokines, therefore presenting a site of direct, complex interaction between the immune system and the tumor cells. In order to analyse the TME`s composition and possible effects of PFK-158 treatment, ascites-derived immune cells were isolated and quantified via flow cytometry. Moreover, cytokines present in the ascites at the time of autopsy were identified and measured via ELISA.

IL-6 showed the highest concentration levels in the ascitic fluid, followed by IL-10 and TNFα. The concentration levels of these cytokines, as well as IL-2, IL-5, IL-10, IL-12p70 and IL-17 remained consistent in the control and treatment group. The previously observed reduction of IL-6 levels in plasma did not occur in the tumor microenvironment.

The levels of IL-4 were significantly reduced by PFK-158 treatment, repeating the findings from plasma analysis. Interestingly, the amount of Th2 cells in ascites has also slightly declined in the treatment group, possibly explaining the drop in its signature cytokine.

Furthermore, the pro-inflammatory IL-1β levels significantly decreased under the influence of glycolytic inhibition.

Finally, the concentration levels of IFNɣ, which were the lowest among all analysed cytokines in the control group, showed a significant increase in the tumor microenvironment of OC under PFK-158 treatment.

A switch in the Th17/Treg ratio observed in the secondary lymphatic organ was not present in the TME, as the amount of Th17, Treg, Th1, CD4+ and CD8+ T cells remained unchanged between the groups.

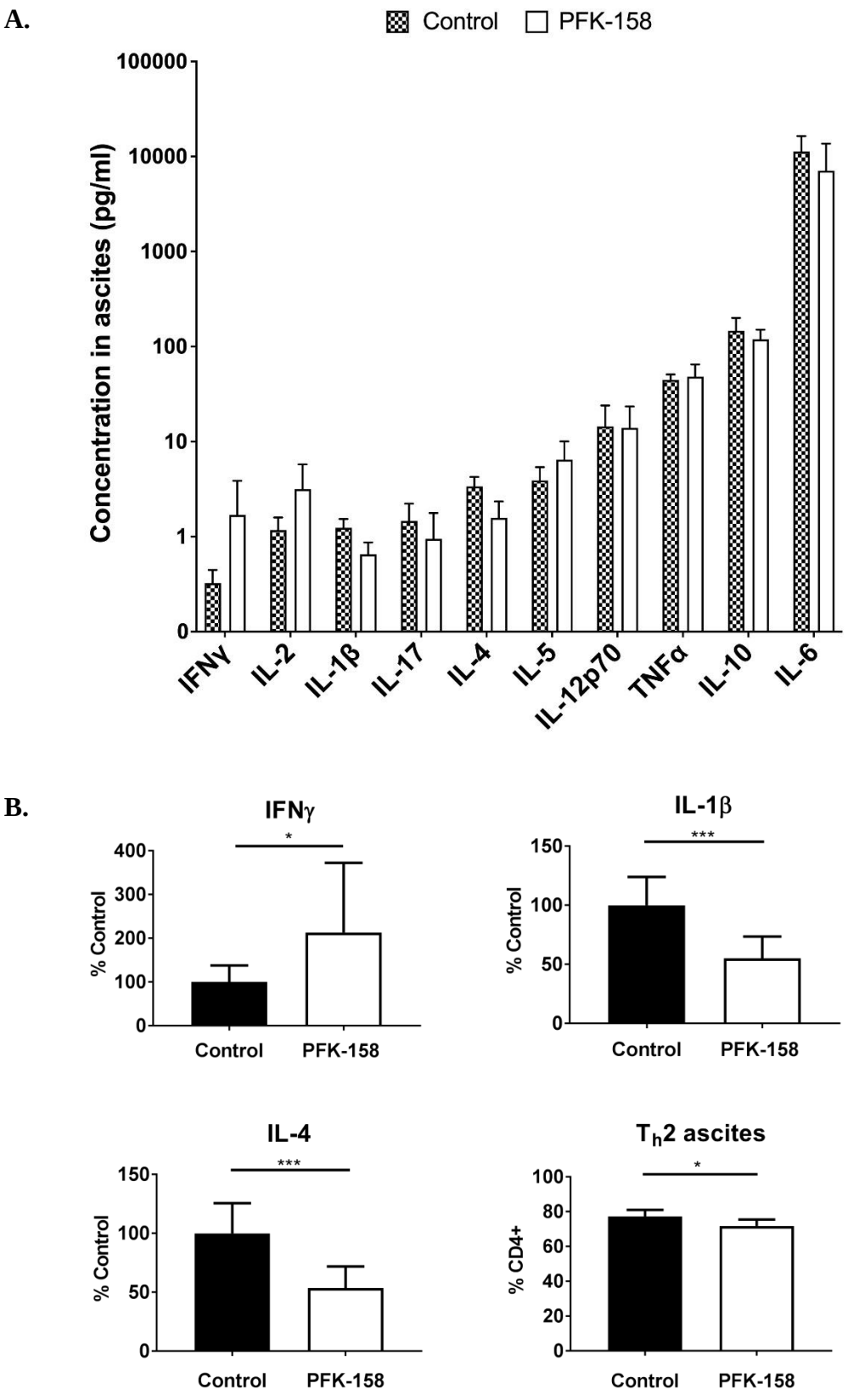

Fig. 20: Cytokine composition in the ascites of treated and untreated mice (absolute concentration levels). Each bar represents the mean ± SD of duplicates for each individual ascites sample per mouse per group (A). Changes in cytokine concentration of IFNγ, IL-1β and IL-4 and Th2 levels in the tumor microenvironment of treated and untreated mice (B); * $p < 0.05$, *** $p < 0.0005$.

VI.3.5 PFK-158 treatment increases the number of tumor-infiltrating CD8+ T cells in tumor-bearing mice.

Finally, the immunohistochemical analysis of tumor-infiltrating CD8+ cytotoxic T cells was performed for both groups. The results showed a significant increase of cytotoxic T cells in the PFK-158 treatment group, as shown below (Fig. 20).

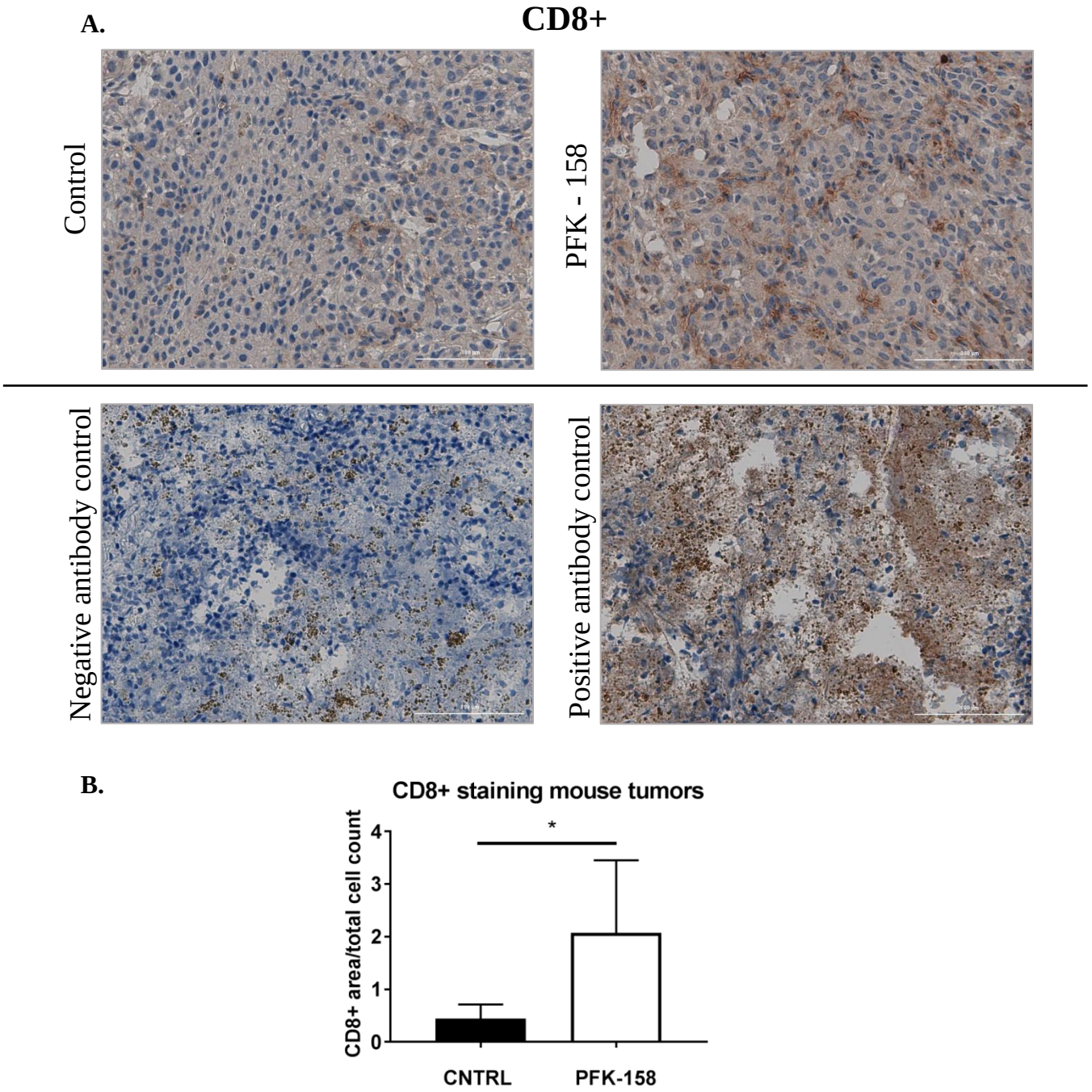

Fig. 21: IHC analysis of tumor-infiltrating CD8+ T cells from vehicle or treated mice (upper row) and negative/positive antibody staining controls (lower row) (A). Scale bar: 100 μm. Quantitative analysis of CD8+ T cells staining in mouse syngeneic tumor tissues across control and treatment groups. Each bar represents the mean ± SD of five independent samples per group, $*p < 0.05$ (B).

VII. Discussion

Despite significant advances in surgery and chemotherapy, ovarian cancer remains the leading cause of death among gynecological malignancies (Khazaei et al., 2021). Since introducing paclitaxel in first-line treatment in 1992, conventional therapies have reached a standstill without any definitive increase in progression-free survival (Odunsi, 2017). In consequence, new treatment strategies are continuously being explored. The dialogue between the immune system and cancer has moved to the forefront of both clinical and basic research following the latest success of cancer immunotherapy. The cause-and-effect relationship between metabolic reprogramming and T-cell-mediated immune response has sparked intense interest and further investigation is being conducted to establish potential new targets for therapy (Renner et al., 2019; Sukumar et al., 2013; Telang et al., 2012). At its` core, this research revolves around the role of glycolysis in the tumorigenic and immunosuppressive process of cancer development and the question of how metabolic alterations might help tumor-resistant T cells overcome those limitations.

An increase in aerobic glycolysis as a result of metabolic reprogramming is commonly known as the Warburg effect and represents a distinctive hallmark of cancer (DeBerardinis & Chandel, 2016; Park, Pyun, & Park, 2020; Ward & Thompson, 2012). The fermentation of glucose provides energy in form of ATP as well as building blocks to support cell proliferation, ensure survival and expand the metastatic potential of malignant cells (Vander Heiden et al., 2009). In addition, aerobic glycolysis is linked to drug resistance in chemotherapy (Zhao, Butler, & Tan, 2013). PFKFB3 is a bifunctional enzyme controlling the synthesis of fructose-2,6-bisphosphate, which in turn activates PFK-1, a critical regulatory molecule in promoting glycolysis (Yalcin, Telang, Clem, & Chesney, 2009). Numerous solid tumors have been shown to have a significantly higher PFKFB3 protein expression (Cantelmo et al., 2016; X. Li et al., 2018; Matsumoto et al., 2021; Xiao et al., 2021; J. Zhang et al., 2020). Therefore, this glycolytic enzyme presents an important metabolic target in cancer therapy overall and in ovarian cancer specifically (Jiang et al., 2022; Mondal et al., 2019; Xintaropoulou et al., 2015; Xintaropoulou et al., 2018).

The Warburg effect, however, is not limited to tumor cell metabolism. It is also a reoccurring phenomenon in T cell activation upon encountering antigen (Andrejeva

& Rathmell, 2017; Icard, Alifano, Donnadieu, & Simula, 2021; Yang, Goronzy, & Weyand, 2014). Antigen recognition triggers T cell differentiation into effector and memory cells, rapid proliferation and the production of various cytokines. In such an energy-demanding state, aerobic glycolysis provides many benefits compared to oxidative proliferation (Cammann et al., 2016; Hume, Radik, Ferber, & Weidemann, 1978; Pearce, 2010): 1). ATP is generated much more rapidly by aerobic glycolysis than oxidation, thus ensuring flexibility and a steady energy supply. 2) Synthesis intermediates for cell proliferation, such as acetyl-CoA, NAPDH, non-essential amino acids and ribosomes are provided as byproducts of glycolysis. 3). This energy-creating pathway allows cells to avoid reactive oxygen species (ROS)-related damage. Previous studies have described a marked increase of PFKFB3 and subsequently F2,6BP expression upon T cell stimulation *ex vivo* (Simon-Molas et al., 2018; Telang et al., 2012; Yang et al., 2014). The commitment to aerobic glycolysis largely depends on the particular function of a specific T cell (Palmer et al., 2015). Therefore, metabolic alterations targeting glycolysis influence T cells differently depending on their subset. As a result, a shift in cellular differentiation and function as well as the cytokine signaling profile toward T cells utilizing oxidative phosphorylation as means of energy supply can be expected (Chang et al., 2013).

Inflammatory conditions present at the tumor site affect the availability and distribution of energy (Fonseca, Farkas, Dora, von Haehling, & Lainscak, 2020; H. Wang & Ye, 2015). Given that the metabolic requirements between cancer and active immune cells are similar, there is constant competition for nutrients in the tumor microenvironment (Andrejeva & Rathmell, 2017; Bi, Bi, Pan, & Yang, 2021). The tumor microenvironment describes a primary or metastatic niche, where tumor cells interact with the host immune system and its metabolites (X. Luo, Xu, Yu, & Yi, 2021). These interactions are vital to orchestrating tumor development, metastasis and eventually immune escape. Malignant ascites is an important part of TME and may provide an immunosuppressive environment (Giuntoli et al., 2009; Kim, Kim, & Song, 2016). For this reason, its` cellular and acellular composition has been of great interest to our *in vivo* research.

Interestingly, a direct comparison of the glycolytic influx and rates of glycolysis between activated and leukemic T cells showed a higher glycolytic metabolism rates in non-malignant T cells (Kishton et al., 2016). Thus, physiological T cells are likely

to out-compete tumor cells in a direct nutrient-based cellular rivalry. In an effort to limit tumor growth, altering the metabolic pathway by the use of a systemic glycolytic inhibitor has already been successfully employed. However, this strategy does not disturb the proliferation of malignant cells selectively, but can in turn also influence T cell activation and functions (Telang et al., 2012). Glucose metabolism is therefore a powerful regulator of the immune response. Glycolysis inhibition by 2-deoxyglucose in CD8+ T cells reduced the cytotoxic activity even though cytokine production remained constant (Finlay, 2015; Renner et al., 2015). Moreover, limiting glucose metabolism in activated T cells induced anergy, an unresponsive state indifferent to antigen encounter, which is also characterized by the inability to proliferate (Zheng, Delgoffe, Meyer, Chan, & Powell, 2009). In fact, glycolytic inhibition has been utilized to suppress T cell responses in autoimmune diseases such as lupus erythematosus, rheumatoid arthritis and diabetes mellitus type 1 (Abboud et al., 2018; W. Li et al., 2019; Martins et al., 2021). Activated T cells play a central role in the efficacy of anti-tumor immune response, hence a delicate equilibrium of pro- and anti-tumor immune signaling needs to be achieved for successful tumor elimination. The effects of PFKFB3 inhibition on this equilibrium have not been previously explored.

This study has demonstrated the ability of PFK-158 to significantly decrease cell viability *in vitro* and inhibit tumorigenic growth in a syngeneic ovarian cancer model as a single agent *in vivo*. The impact of targeted PFKFB3 inhibition on reducing tumor burden has been previously described in several gynecological and other malignancies (Cargill et al., 2021; Guan et al., 2020; Mondal et al., 2019; Ray et al., 2021; Sarkar Bhattacharya et al., 2019; Xiao et al., 2021). In endometrial and ovarian cancer, PFK-158 has been used alone and in combination with carboplatin and was shown to exhibit a synergistic activity. This combination strategy enhanced chemosensitivity of cancer cells, as well as induced apoptosis and autophagy by the Akt/mTOR signaling and downregulation of the p62/SQSTM1 mechanism (Mondal et al., 2019; Xiao et al., 2021). The Akt/mTOR signalling pathway is frequently overexpressed in women suffering from OC (Ediriweera, Tennekoon, & Samarakoon, 2019; Ghoneum, Abdulfattah, & Said, 2020). It has been linked to poor prognosis through accelerated proliferation and chemoresistance of tumor cells and

aggressively pursued as a target for new drug development (Mabuchi, Kuroda, Takahashi, & Sasano, 2015).

Although a combination of PFK-158 with carboplatin or paclitaxel appears to yield the best clinical results, we specifically focused our research on the single agent strategy for two main reasons: 1). In order to properly assess cytoreductive properties of isolated glycolytic inhibition without relying on the established first-line therapy regimen and 2). In an effort to assess the effects of PFKFB3 inhibition in a model with direct competition for nutrients between tumor and immune cells while avoiding other pharmacological influences. As the majority of metastatic disease in OC is confined to the peritoneal cavity, intraperitoneal drug administration has allowed for a targeted therapy approach directly to the tumor site, minimizing potential systemic damage. This technique has been shown to prolong the overall survival in patients with stage III ovarian cancer, who could also tolerate the aggressive side effects of this treatment (Armstrong et al., 2006; Marchetti et al., 2019).

We have shown that PFK-158 inhibits T cell viability, proliferation and function by directly inhibiting PFKFB3 and reducing intracellular glucose uptake *ex vivo.* A reduced glucose uptake appeared to be associated with a drop in ATP generation, though without reaching statistical significance. Telang et al. presented similar results in the 2012 study aiming at F2,6BP inhibition in T cells in a psoriasis mouse model (Telang et al., 2012). While the overall cytokine levels of IL-10, IL-4, IL-17 and IFN-ɣ in our experiment decreased in a dose-dependent manner, the analysis of cytokine production per single T cell revealed a lesser, mostly dose-independent decline. Consequently, the inhibition of T cell function can be generally attributed to a drop in viable T cells, while the surviving cells remain functionally active. Moreover, by including a rehabilitation period following PFK-158 treatment, we have demonstrated that the loss of T cell function was reversible in groups treated with a low PFK-158 dosage. According to the patent, the half-life of the compound has been determined at 10.5 hours (Gilles H. Tapolsky, 2017), which might account for quick T cell regeneration in an *ex vivo* setting. Additionally, although glycolysis is the predominant pathway to energy in the activated state, OXPHOS remains functional in T cells (Luby & Alves-Guerra, 2021).

Lastly, we observed, that i.p. administration of a well-tolerated dose of PFK-158 suppressed tumor growth while boosting infiltration of T cells into tumor tissue, increasing the concentration of IFN-ɣ in ascites and decreasing the concentration of the pro-inflammatory IL-6 in murine plasma *in vivo.* All prior studies involving PFK-158 were performed using immunodeficient athymic nude mice, thereby limiting research directed at the immunological aspects of these metabolic alterations in cancer. In fact, no studies to date have demonstrated the effect of PFKFB3 inhibition on the T-cell-mediated anti-tumor response. For the first time, the effects of PFK-158 have been studied in an immunocompetent mouse model, therefore allowing for observations regarding the immune response. We focused our attention specifically on the adaptive immune cell subsets and cytokine levels, which have been shown to have prognostic value in OC. The results of this research reveal the potential utility of targeting glycolytic inhibition as a part of a therapeutic strategy. (Ediriweera et al., 2019).

Multiple independent studies have identified a number of specific markers for an effective anti-tumor immune response and therefore better patient outcome in OC. The most relevant cellular prognostic factor in advanced OC is the presence of tumor-infiltrating lymphocytes (TIL). Specifically, CD8+ cytotoxic T cells are the most powerful anti-tumor effector cells and represent the cornerstone of cancer immunotherapy (Raskov, Orhan, Christensen, & Gögenur, 2021). Our research has demonstrated a significant increase in CD8+ cytotoxic T cells infiltrating tumor islets of PFK-158 treated mice. In a 2003 published paper, Zhang et al. were the first to establish a correlation between TILs presence and improved clinical outcome in the advanced stages of the disease (L. Zhang et al., 2003). In the following years, more evidence was collected in support of this finding (Gavalas et al., 2010; J. Li, Wang, Chen, Bai, & Lu, 2017; Santoiemma & Powell, 2015; Sato et al., 2005; Tomsová, Melichar, Sedláková, & Steiner, 2008; W. Wang et al., 2018). Together, these studies support the hypothesis, that tumor infiltration by CD8+ lymphocytes directly mirrors the tumor-related immune response (Odunsi, 2017). A 2012 published meta-analysis of 10 studies involving 1815 patients translated data from basic research into clinically relevant survival statistics - women with ovarian cancers lacking intra-epithelial TILs were 1.53 times more at risk of dying than women with tumors containing $CD8^+$ TILs (Hwang et al., 2012). According to Zhang et al., the 5-

year progress-free survival for patients with TILs was 38% compared to 4.5% in patients whose tumors did not contain T cell islets (L. Zhang et al., 2003). Based on a mouse model, anti-tumor functionality was shown to improve in CD8+ cells through specific inhibition of glycolytic flux by 2-deoxyglucose (Sukumar et al., 2013). While CD8+ T cells with a glycolytic phenotype were likely to be short-lived, a low glycolytic activity helped to form long-lasting memory T cells, thus improving efficacy. In a 2014 published comment, the authors conclude that antiglycolytic treatment results in a less acidic microenvironment due to a reduction in lactate output, leading to a removal of a blockade against TILs while simultaneously hindering tumor progression (Karthikeyan, Geschwind, & Ganapathy-Kanniappan, 2014).

An effective anti-tumor immune response cannot solely rely on cytotoxic CD8+ T cells, but optimally requires equal CD4+ T cell participation, as they contribute pro-inflammatory signals via crucial cytokine production. Several studies attributed a positive influence of elevated IFN-ɣ levels in the ascitic fluid to a more favorable prognosis. IFN-ɣ is a central effector molecule of CD4+ and CD8+ T cells with a broad range of activity, such as the recruitment of neutrophils to the site of infection and up-regulation of MHC class I expression as well as antigen processing (Ellis & Beaman, 2004; Zhou, 2009). It has been shown to activate tumor-associated macrophages and to enhance their tumor lysing abilities, hereby transforming the tumor microenvironment from immunosuppressive to immunostimulatory and contributing to the reduction of ovarian tumor growth (Spear, Barber, Rynda-Apple, & Sentman, 2012). Sun et al. recently combined monophosphoryl lipid A with IFN-ɣ in an i.p. injection to reprogram tumor-associated macrophages into tumoricidal macrophages, thereby eliciting a significant anti-metastatic response and enhancing chemosensitivity in a mouse model (Sun et al., 2021). Green et al. have used a combination treatment with IL-4, IFN-α and IFN-ɣ to successfully prolong overall survival of mice with human ovarian cancer xenograft (Green et al., 2019). IFN-ɣ has also been demonstrated to possess direct antiproliferative activity and induce apoptosis in human OC cells in vivo (Wall et al., 2003). In vitro, continuous exposure to IFN-ɣ led to irreversible inhibition in cell growth through a sustained induction of p21 and IRF-1 (Burke, Smith, Crompton, Upton, & Balkwill, 1999). A more recent study attributed the same effect to the suppression of STAT3 and STAT5 protein

phosphorylation, which negatively affected cell migration and invasion, as well as prevented cell transition from G0/G1 to S phase and enhanced apoptosis (Gao et al., 2022). Alterations in T cell metabolism and its` influence on IFN-ɣ secretion have also yielded noteworthy results. Interestingly, 2015 and 2019 published research revealed, that depriving human T cells of glucose did not result in decreased levels of IFN-ɣ *in vitro*, indicating certain metabolic plasticity of T cells under nutritional stress (Renner et al., 2019; Renner et al., 2015). Direct glycolytic inhibition by 2-deoxyglucose significantly impaired the effector function of T cells as measured by IFN-ɣ production, which persisted after 2-deoxyglucose pretreated T-cell cultures were washed and restimulated in the absence of the inhibitor. These findings are contradictory to our *ex vivo* and *in vivo* data, as a continuous drop in IFN-ɣ was not observed. In contrast, we detected elevated levels of IFN-ɣ, as secreted per live T cell following PFK-158 treatment in *ex vivo* conditions, as well as higher concentrations in the ascites of the treated mouse group. A possible explanation lies in the dual inhibitory properties of 2-deoxyglucose – further analysis revealed that it impairs glycolytic activity and simultaneously reduces mitochondrial respiration in human T cells (Renner et al., 2015). PFK-158, however, is a specific inhibitor of PFKFB3, which does not influence any metabolic pathways outside of glycolysis. It is conceivable, that inhibiting T cell glycolysis may push T cells into a metabolic switch to OXPHOS, thereby maintaining their functional and proliferative qualities. Salerno et al. further support this theory by concluding that the production of IFNɣ by CD8+ T cells is independent of glycolysis but rather relies on mitochondrial respiration (Salerno, Guislain, Cansever, & Wolkers, 2016).

Furthermore, the comparative analysis of ascites and plasma from treated and untreated mice revealed no major changes in the number of T cell subpopulations between the two groups despite targeted glycolytic inhibition. The only significant difference was observed in the ascitic Th2 subset levels, which were slightly reduced in the treatment group. A quantitative alteration of the T cell profile is not correlated with clinical tumor characteristics or patient outcome (Wefers et al., 2018). However, the effector function of Th2 cells, as measured by their signature cytokine IL-4, possesses some prognostic value. Th1 response linked cytokines are expected to predict better patient outcome, while those representing the Th2 response have been linked to unsatisfactory cytoreductive surgery results and undifferentiated

tumors (Cândido et al., 2013; Gavalas et al., 2010). Unlike IFN-ɣ, IL-4 is attributed to inhibitory cytokines, which hamper the cell-mediated immune response to the presence of cancer cells (Baci et al., 2020; Giuntoli et al., 2009). Our study has revealed a significant decline in IL-4 levels in the ascitic fluid as well as in murine serum after treatment with PFK-158. Chen et al. concluded, that IL-4 can be independently produced by epithelial ovarian carcinoma cells themselves, which contributes to the development of immune deficiency in the peritoneal cavity of EOC patients (L. L. Chen et al., 2009). In plasma, patients with advanced serous ovarian cancer exhibited elevated IL-4 serum levels compared to healthy controls (Zhu, Ying, Xu, Zhu, & Xie, 2010). Therefore, reducing the concentration may contribute to reversing the immunosuppressive impact of IL-4 in ovarian cancer-associated ascites and plasma.

Another prognostic inflammatory cytokine known to be crucially involved in tumor proliferation and invasive cell behaviour is IL-1 (Z. Chen et al., 2001; Marth et al., 1996). Stromal IL-1β secreted by OC cells was shown to suppress p53 protein expression in cancer-associated fibroblasts, thereby promoting tumorigenesis and resulting in reduced overall patient survival (Schauer et al., 2013). Moreover, IL-1β was identified as a possible trigger for ascitic VEGF and mesothelial cell β1-integrin production, facilitating angiogenesis and tumor dissemination (Stadlmann et al., 2005; Watanabe et al., 2012). Another study by Woolery et al. concluded, that BRCA1-mutated ovarian cells, associated with an increased risk of developing OC, enhanced the expression of IL-1β (Woolery et al., 2015). In our study, selective PFKFB3-inhibition resulted in significantly decreased levels of IL-1β in TME, suggesting a beneficial shift in the anti-tumor immune response.

When comparing the serum samples of the control and treatment groups, a change in IL-6 plasma cytokine levels was detected. Despite no changes in ascites levels, the plasma levels of IL-6 presented a significant decrease under glycolytic inhibition. IL-6 is a multifunctional cytokine produced by various cell types, such as lymphocytes, monocytes and epithelial cells, as well as by ovarian carcinoma cells in response to inflammatory signals (Schröder, Ruppert, & Bender, 1994; Szulc-Kielbik, Kielbik, Nowak, & Klink, 2021). The wide range of its effects includes the induction of B- and T-cell differentiation and acute phase reactant, but it may also act as a growth factor for malignancy (Berek et al., 1991). Serum IL-6 is commonly investigated in OC

patients for its prognostic value, as its concentration in healthy individuals is very low (5pg/ml), but can increase significantly under inflammatory conditions triggered by tumor progression (Szulc-Kielbik et al., 2021). Several studies have shown a significant association between higher IL-6 levels in ascites and serum of OC patients and poor overall survival (Berek et al., 1991; Dobrzycka et al., 2013; J. H. Luo et al., 2017; Sanguinete et al., 2017; Scambia et al., 1995; Tempfer et al., 1997). The mechanisms by which IL-6 participates in OC progression are complex and involve the response of both immune and cancer cells to its` signalling. 1). IL-6 promotes OC proliferation and growth while simultaneously inhibiting the apoptosis of cancer cells (Dijkgraaf, Welters, Nortier, van der Burg, & Kroep, 2012; Y. Wang et al., 2005). 2). The proinflammatory cytokine promotes angiogenesis and with it OC metastasis (Browning, Patel, Horvath, Tawara, & Jorcyk, 2018). 3). IL-6 drives chemoresistance in OC (Niu, Yao, Bast, Sood, & Liu, 2021; Yousefi et al., 2018). The value of IL-6 as a reliable biomarker has been largely debated. While some studies stated, that IL-6 is a good predictive biomarker, it was not found to be superior to conventional tests, like CA125 (Kampan et al., 2020). Moreover, Lambeck et al., Sen et al. and Block et al. concluded that IL-6 is insufficient as a sole biomarker in OC but may still play a role in diagnostics by distinguishing between benign and malignant tissue (Block et al., 2015; Lambeck et al., 2007; Sen et al., 2011). The importance of IL-6 is underlined in research studying this cytokine as a potential target for anti-cancer therapy. Neutralizing this cytokine significantly enhanced the therapeutic efficacy of paclitaxel and was shown to reduce tumor growth and angiogenesis (Coward et al., 2011; Dijkgraaf et al., 2012; Rossi, Lu, Jourdan, & Klein, 2015; R. Zhang, Roque, Reader, & Lin, 2022). Taken together, the results of our study indicate that reducing IL-6 serum levels may positively contribute to hampering disease progression and increase overall survival.

Lastly, our results show that there was no influence of PFK-158 treatment on IL-17 concentration levels in the TME or serum. PFKFB3 inhibition, however, led to a reciprocal conversion of Th17 into Treg cells in the lymphocytic population of the spleen. Ye et al. have described the developmental plasticity between these two CD4+ T cell subtypes, as they possess the capacity to interchangeably differentiate into each other, and showed that the T cell receptor (TCR) was responsible for this transformation (Ye et al., 2011). High levels of glycolytic activity are found in Th1,

Th2 and Th17 effector T cells as they transition from the OXPHOS-dominant catabolic phenotype to glucose-driven anabolic phenotype upon activation (Shen & Shi, 2019). Tregs display elevated rates of lipid oxidation instead (Michalek et al., 2011). Accordingly, blocking glycolysis with 2-deoxyglucose inhibits Th17 differentiation and promotes Treg formation (Shi et al., 2011). In OC, Th17 T lymphocytes are the sole source of IL-17, a cytokine responsible for the migration of neutrophils and initiation of an inflammatory reaction (Rogala et al., 2011; Wilke et al., 2011), and also required in the recruitment and tumor-promoting activity of MDSC (Charles et al., 2009; He et al., 2010). Interestingly, despite the changed cellular composition of the spleen, IL-17 levels remained unaffected by PFK-158 treatment in the TME and serum of tumor bearing mice. Collectively, these findings provide a possible explanation for the Th17/Treg ratio switch due to the metabolic changes induced by PFK-158. However, since his switch was exclusively observed in the spleen but not the TME or tumor islets and had no influence on the expression levels of IL-17 at tumor site, the clinical relevance remains yet to be determined.

In addition to differences in cellular composition and humoral signalling, the autopsy revealed macroscopic alterations visible in the abdominal organs of the treated mice. Interestingly, chronic mesenteritis could be observed in one mouse sacrificed five days before the end of the experiment, as was reviewed in the pathology evaluation (for detailed information, see supplementary data). Unlike the control group, the majority of treated mice displayed distended intestines mostly located in the right lower abdominal flank i.e. injection site. While the rationale for this incidental finding is not immediately apparent, a 2015 study has linked the impairment of glucose metabolism to sclerosing mesenteritis development (Pereira et al., 2015). Further research is necessary to establish a possible relationship between PFK-158 treatment and abdominal distension, mesenteritis and intestinal ulceration. However, it was not the main focus of this particular study.

A predominant aspect in the research of PFKFB3 inhibition is its influence on overall survival in immunocompetent mice. Previous studies of our working group suggest a survival benefit for groups either treated with PFK-158 alone or undergoing a combination therapy with carboplatin in nude mice (Mondal et al., 2019; Xiao et al., 2021). A survival analysis using immunocompetent mice with OC under PFK-158

treatment was not yet performed and could present a valuable source of information in future research.

In conclusion, this study is the first to investigate the synergistic anti-tumor and immune-modulating effects of PFK-158, a specific inhibitor of PFKFB3, in a syngeneic OC model. The results of this study strongly indicate a shift towards a more potent pro-inflammatory immune response in the presence of malignant cells, suggesting a potential benefit in targeting the glycolytic pathway as a novel therapeutic option for patients with advanced stage OC.

VIII. Summary

Background: Despite significant advances in surgery and chemotherapy, ovarian cancer remains the leading cause of death among gynecological malignancies. In an effort to establish new therapies, the focus has shifted toward restricting cancer metabolism. A key regulatory enzyme, PFKFB3, is overexpressed in OC and plays an important role in promoting tumor cell growth. Targeting glycolysis via selective PFKFB3 inhibition has shown promising results in pre-clinical studies. Nevertheless, its effects on the hosts` ability to initiate a potent anti-tumor immune response remain unknown. In this study, we describe the effects of PFK-158, a novel selective molecule inhibitor of PFKFB3, on the immune profile of mice using a syngeneic ovarian cancer model.

Methods: We investigated the anti-cancer activity and immune-modulating effects of PFK-158 treatment *in vitro, ex vivo* and *in vivo*. The focus of this study has been the adaptive immune system and more specifically, the T cell mediated immune response, being the most relevant prognostic factor in OC survival. Proliferation and metabolomic analysis were performed on serous ovarian cancer mimicking STOSE cells as well as murine T cells purified from splenic tissue. T cell secretory function was assessed by flow cytometry. Lastly, a comparative analysis of tumor burden and immunologic parameters in plasma, spleens and ascitic fluid was performed in the control and treatment groups.

Results: Our study showed that PFKFB3 inhibition decreased the proliferation of malignant cells by metabolic restriction *in vitro* and resulted in suppressed tumor growth *in vivo*. PFK-158 also inhibited T cell viability, proliferation and function as measured by cytokine release *ex vivo*. However, the loss of function proved to be reversible following a drug-free rehabilitation phase. Most importantly, we observed, that i.p. administration of PFK-158 led to elevated concentration levels of the immune-activating cytokine IFN-ɣ, while the concentration of immune-suppressing anti-inflammatory cytokines IL-4 and IL-6 declined *in vivo.* Moreover, immunohistochemical examination of the tumor tissue samples revealed an increase in tumor-infiltrating CD8+ lymphocytes under PFK-158 treatment.

Conclusion: Our research demonstrates that direct PFKFB3 inhibition not only impairs tumor growth via metabolic restrain in OC but also leads to tipping the scales towards a more effective anti-tumor immune response.

IX. Zusammenfassung

Hintergrund: Trotz beachtlicher Erfolge im operativen und chemotherapeutischen Bereich ist das Ovarialkarzinom nach wie vor die häufigste Todesursache unter den malignen gynäkologischen Erkrankungen. Bei den Bestrebungen, neue Therapiekonzepte zu entwickeln, verlagerte sich der Fokus auf metabolische Tumorrestriktion. Ein regulierendes Schlüsselenzym, PFKFB3, ist überexprimiert im Ovarialkarzinom und fördert das Tumorwachstum. Die selektive Hemmung der Glykolyse über das PFKFB3-Enzym zeigte vielversprechende Ergebnisse in präklinischen Studien. Nichtsdestotrotz sind dessen Effekte auf das Generieren einer effektiven Tumor-assoziierten Immunantwort kaum erforscht. In dieser Arbeit werden die Einflüsse von PFK-158, einem selektiven molekularen PFKFB3-Inhibitor, auf das Immunprofil von Mäusen in einem syngenen Ovarialkarzinommodel beschrieben.

Methoden: In der vorliegenden Dissertation wurden die Antitumor-Aktivität und immunmodulierende Effekte der Behandlung mit PFK-158 *in vitro, ex vivo* und *in vivo* dargestellt. Im Mittelpunkt der Studie stand dabei das adaptive Immunsystem und speziell die T-Zell-vermittelte Immunabwehr, da diese den wichtigsten prognostischen Faktor beim Ovarialkarzinom abbildet. Proliferations- und metabolische Analysen wurden an STOSE-Zellen, welche das seröse Ovarialkarzinom imitieren, sowie an murinen T-Lymphozyten der Milz durchgeführt. Die Sekretionsfunktion der T-Zellen wurde mittels Durchflusszytometrie beurteilt. Zuletzt wurde eine Vergleichsanalyse in Bezug auf Tumormasse und Immunparametern in Plasma, Milz und Aszitesflüssigkeit zwischen der Kontroll- und Behandlungsgruppe erstellt.

Ergebnisse: Diese wissenschaftliche Arbeit hat gezeigt, dass PFKFB3-Inhibierung die Vermehrung maligner Zellen mittels metabolischer Restriktion *in vitro* hemmt und das Tumorwachstum *in vivo* unterdrückt. PFK-158 inhibierte zudem die T-Zell-Überlebensfähigkeit, -Proliferation und –Funktion, welche mittels Zytokinsekretion *ex vivo* gemessen wurde. Der Funktionsverlust konnte jedoch nach anschließender Rehabilitationsphase ohne Inhibitor überwunden werden. Als bedeutendstes Ergebnis dieser Arbeit haben die *in vivo* Studien gezeigt, dass intraperitoneale PFK-158-Injektionen zu erhöhten Konzentrationen des immunstimulierenden Zytokins IFN-ɣ geführt haben, währen die Konzentrationen der immunhemmenden Zytokine IL-4 und IL-6 abnahmen. Darüber hinaus zeigte die immunhistochemische Untersuchung der

Tumorproben eine erhöhte Infiltration des Tumorgewebes mit CD8+ zytotoxischen T Lymphozyten unter der Therapie mit PFK-158.

Schlussfolgerung: Zusammenfassend demonstriert diese Studie, dass direkte PFKFB3-Inhibierung im Ovarialkarzinom nicht nur das Tumorwachstum mittels metabolischer Restriktion unterdrückt, sondern auch zu einer Verlagerung des immunologischen Gleichgewichts zugunsten einer effektiveren Anti-Tumor-Immunantwort führt.

X. References

Abboud, G., Choi, S. C., Kanda, N., Zeumer-Spataro, L., Roopenian, D. C., & Morel, L. (2018). Inhibition of Glycolysis Reduces Disease Severity in an Autoimmune Model of Rheumatoid Arthritis. *Frontiers in Immunology, 9*, 1973. doi:10.3389/fimmu.2018.01973

Andrejeva, G., & Rathmell, J. C. (2017). Similarities and Distinctions of Cancer and Immune Metabolism in Inflammation and Tumors. *Cell Metabolism, 26*(1), 49-70. doi:10.1016/j.cmet.2017.06.004

Armstrong, D. K., Bundy, B., Wenzel, L., Huang, H. Q., Baergen, R., Lele, S., . . . Burger, R. A. (2006). Intraperitoneal cisplatin and paclitaxel in ovarian cancer. *New England Journal of Medicine, 354*(1), 34-43.

Atsumi, T., Chesney, J., Metz, C., Leng, L., Donnelly, S., Makita, Z., . . . Bucala, R. (2002). High Expression of Inducible 6-Phosphofructo-2-Kinase/Fructose-2,6-Bisphosphatase (iPFK-2; PFKFB3) in Human Cancers. *Cancer Research, 62*(20), 5881-5887.

Baci, D., Bosi, A., Gallazzi, M., Rizzi, M., Noonan, D. M., Poggi, A., . . . Mortara, L. (2020). The Ovarian Cancer Tumor Immune Microenvironment (TIME) as Target for Therapy: A Focus on Innate Immunity Cells as Therapeutic Effectors. *International Journal of Molecular Sciences, 21*(9). doi:10.3390/ijms21093125

Bai, H., Cao, D., Yang, J., Li, M., Zhang, Z., & Shen, K. (2016). Genetic and epigenetic heterogeneity of epithelial ovarian cancer and the clinical implications for molecular targeted therapy. *Journal of Cellular and Molecular Medicine, 20*(4), 581-593.

Bando, H., Atsumi, T., Nishio, T., Niwa, H., Mishima, S., Shimizu, C., . . . Koike, T. (2005). Phosphorylation of the 6-phosphofructo-2-kinase/fructose 2,6-bisphosphatase/PFKFB3 family of glycolytic regulators in human cancer. *Clinical Cancer Research, 11*(16), 5784-5792. doi:10.1158/1078-0432.Ccr-05-0149

Berek, J. S., Chung, C., Kaldi, K., Watson, J. M., Knox, R. M., & Martínez-Maza, O. (1991). Serum interleukin-6 levels correlate with disease status in patients with epithelial ovarian cancer. *American Journal of Obstetrics and Gynecology, 164*(4), 1038-1043. doi:10.1016/0002-9378(91)90582-c

Bi, J., Bi, F., Pan, X., & Yang, Q. (2021). Establishment of a novel glycolysis-related prognostic gene signature for ovarian cancer and its relationships with immune infiltration of the tumor microenvironment. *Journal of Translational Medicine, 19*(1), 382. doi:10.1186/s12967-021-03057-0

Block, M. S., Maurer, M. J., Goergen, K., Kalli, K. R., Erskine, C. L., Behrens, M. D., . . . Knutson, K. L. (2015). Plasma immune analytes in patients with epithelial ovarian cancer. *Cytokine, 73*(1), 108-113. doi:10.1016/j.cyto.2015.01.035

Browning, L., Patel, M. R., Horvath, E. B., Tawara, K., & Jorcyk, C. L. (2018). IL-6 and ovarian cancer: inflammatory cytokines in promotion of metastasis. *Cancer Management and Research, 10,* 6685-6693. doi:10.2147/cmar.S179189

Burges, A., & Schmalfeldt, B. (2011). Ovarian cancer: diagnosis and treatment. *Deutsches Arzteblatt International, 108*(38), 635-641. doi:10.3238/arztebl.2011.0635

Burke, F., Smith, P. D., Crompton, M. R., Upton, C., & Balkwill, F. R. (1999). Cytotoxic response of ovarian cancer cell lines to IFN-gamma is associated with sustained induction of IRF-1 and p21 mRNA. *British Journal of Cancer, 80*(8), 1236-1244. doi:10.1038/sj.bjc.6690491

Cammann, C., Rath, A., Reichl, U., Lingel, H., Brunner-Weinzierl, M., Simeoni, L., . . . Lindquist, J. A. (2016). Early changes in the metabolic profile of activated CD8(+) T cells. *BMC Cell Biology, 17*(1), 28. doi:10.1186/s12860-016-0104-x

Cândido, E. B., Silva, L. M., Carvalho, A. T., Lamaita, R. M., Filho, R. M. P., Cota, B. D. C. V., & da Silva-Filho, A. L. (2013). Immune Response Evaluation Through Determination of Type 1, Type 2, and Type 17 Patterns in Patients With Epithelial Ovarian Cancer. *Reproductive Sciences, 20*(7), 828-837. doi:10.1177/1933719112466299

Cantelmo, A. R., Conradi, L. C., Brajic, A., Goveia, J., Kalucka, J., Pircher, A., . . . Carmeliet, P. (2016). Inhibition of the Glycolytic Activator PFKFB3 in Endothelium Induces Tumor Vessel Normalization, Impairs Metastasis, and Improves Chemotherapy. *Cancer Cell, 30*(6), 968-985. doi:10.1016/j.ccell.2016.10.006

Cargill, K. R., Stewart, C. A., Park, E. M., Ramkumar, K., Gay, C. M., Cardnell, R. J., . . . Byers, L. A. (2021). Targeting MYC-enhanced glycolysis for the treatment of small cell lung cancer. *Cancer Metabolism, 9*(1), 33. doi:10.1186/s40170-021-00270-9

Chang, C. H., Curtis, J. D., Maggi, L. B., Jr., Faubert, B., Villarino, A. V., O'Sullivan, D., . . . Pearce, E. L. (2013). Posttranscriptional control of T cell effector function by aerobic glycolysis. *Cell, 153*(6), 1239-1251. doi:10.1016/j.cell.2013.05.016

Charles, K. A., Kulbe, H., Soper, R., Escorcio-Correia, M., Lawrence, T., Schultheis, A., . . . Hagemann, T. (2009). The tumor-promoting actions of TNF-alpha involve TNFR1 and IL-17 in ovarian cancer in mice and humans. *The Journal of Clinical Investigation, 119*(10), 3011-3023. doi:10.1172/jci39065

Chen, L. L., Ye, F., Lü, W. G., Yu, Y., Chen, H. Z., & Xie, X. (2009). Evaluation of immune inhibitory cytokine profiles in epithelial ovarian carcinoma. *The Journal of Obstetrics and Gynaecology Research, 35*(2), 212-218. doi:10.1111/j.1447-0756.2008.00935.x

Chen, Z., Fadiel, A., Feng, Y., Ohtani, K., Rutherford, T., & Naftolin, F. (2001). Ovarian epithelial carcinoma tyrosine phosphorylation, cell proliferation, and ezrin translocation are stimulated by interleukin 1alpha and epidermal growth factor. *Cancer, 92*(12), 3068-3075. doi:10.1002/1097-0142(20011215)92:12<3068::aid-cncr10149>3.0.co;2-5

Clem, B., Telang, S., Clem, A., Yalcin, A., Meier, J., Simmons, A., . . . Chesney, J. (2008). Small-molecule inhibition of 6-phosphofructo-2-kinase activity suppresses glycolytic flux and tumor growth. *Molecular Cancer Therapeutics, 7*(1), 110-120. doi:10.1158/1535-7163.Mct-07-0482

Cori, C. F., & Cori, G. T. (1925). The carbohydrate metabolism of tumors. I. The free sugar, lactic acid, and glycogen content of malignant tumors. *Journal of Biological Chemistry, 64*(11).

Coward, J., Kulbe, H., Chakravarty, P., Leader, D., Vassileva, V., Leinster, D. A., . . . Balkwill, F. R. (2011). Interleukin-6 as a therapeutic target in human ovarian cancer. *Clinical Cancer Research, 17*(18), 6083-6096. doi:10.1158/1078-0432.Ccr-11-0945

Dang, E. V., Barbi, J., Yang, H. Y., Jinasena, D., Yu, H., Zheng, Y., . . . Pan, F. (2011). Control of T(H)17/T(reg) balance by hypoxia-inducible factor 1. *Cell, 146*(5), 772-784. doi:10.1016/j.cell.2011.07.033

DeBerardinis, R. J., & Chandel, N. S. (2016). Fundamentals of cancer metabolism. *Science Advances, 2*(5), e1600200. doi:10.1126/sciadv.1600200

Del Bufalo, D., Biroccio, A., Soddu, S., Laudonio, N., D'Angelo, C., Sacchi, A., & Zupi, G. (1996). Lonidamine induces apoptosis in drug-resistant cells independently of the p53 gene. *The Journal of Clinical Investigation, 98*(5), 1165-1173. doi:10.1172/jci118900

Dijkgraaf, E. M., Welters, M. J., Nortier, J. W., van der Burg, S. H., & Kroep, J. R. (2012). Interleukin-6/interleukin-6 receptor pathway as a new therapy target in epithelial ovarian cancer. *Current Pharmaceutical Design, 18*(25), 3816-3827. doi:10.2174/138161212802002797

Dobrzycka, B., Mackowiak-Matejczyk, B., Terlikowska, K. M., Kulesza-Bronczyk, B., Kinalski, M., & Terlikowski, S. J. (2013). Serum levels of IL-6, IL-8 and CRP as prognostic factors in epithelial ovarian cancer. *European Cytokine Network, 24*(3), 106-113. doi:10.1684/ecn.2013.0340

Dunn, G. P., Old, L. J., & Schreiber, R. D. (2004). The three Es of cancer immunoediting. *Annual Reviev of Immunology, 22*, 329-360. doi:10.1146/annurev.immunol.22.012703.104803

Ediriweera, M. K., Tennekoon, K. H., & Samarakoon, S. R. (2019). Role of the PI3K/AKT/mTOR signaling pathway in ovarian cancer: Biological and

therapeutic significance. *Seminars in Cancer Biology, 59*, 147-160. doi:10.1016/j.semcancer.2019.05.012

Ellis, T. N., & Beaman, B. L. (2004). Interferon-gamma activation of polymorphonuclear neutrophil function. *Immunology, 112*(1), 2-12. doi:10.1111/j.1365-2567.2004.01849.x

Finlay, D. K. (2015). Starved human T lymphocytes keep fighting. *European Journal of Immunology, 45*(9), 2480-2483. doi:10.1002/eji.201545885

Fonseca, G., Farkas, J., Dora, E., von Haehling, S., & Lainscak, M. (2020). Cancer Cachexia and Related Metabolic Dysfunction. *International Journal of Molecular Sciences, 21*(7). doi:10.3390/ijms21072321

Fox, C. J., Hammerman, P. S., & Thompson, C. B. (2005). Fuel feeds function: energy metabolism and the T-cell response. *Nature Reviews. Immunology, 5*(11), 844-852. doi:10.1038/nri1710

Gamwell, L. F., Collins, O., & Vanderhyden, B. C. (2012). The mouse ovarian surface epithelium contains a population of LY6A (SCA-1) expressing progenitor cells that are regulated by ovulation-associated factors. *Biology of Reproduction, 87*(4), 80. doi:10.1095/biolreprod.112.100347

Ganapathy-Kanniappan, S., & Geschwind, J. F. (2013). Tumor glycolysis as a target for cancer therapy: progress and prospects. *Molecular Cancer, 12*, 152. doi:10.1186/1476-4598-12-152

Gao, A. H., Hu, Y. R., & Zhu, W. P. (2022). IFN-γ inhibits ovarian cancer progression via SOCS1/JAK/STAT signaling pathway. *Clinical & Translational Oncology, 24*(1), 57-65. doi:10.1007/s12094-021-02668-9

Gavalas, N. G., Karadimou, A., Dimopoulos, M. A., & Bamias, A. (2010). Immune Response in Ovarian Cancer: How Is the Immune System Involved in Prognosis and Therapy: Potential for Treatment Utilization. *Clinical and Developmental Immunology, 2010*, 791603. doi:10.1155/2010/791603

Ghoneum, A., Abdulfattah, A. Y., & Said, N. (2020). Targeting the PI3K/AKT/mTOR/NFκB Axis in Ovarian Cancer. *Journal of Cellular Immunology, 2*(2), 68-73. doi:10.33696/immunology.1.022

Gilles H. Tapolsky, P. C. (2017). United Ustates of America Patent No. US20150064175A1.

Giuntoli, R. L., WEBB, T. J., ZOSO, A., ROGERS, O., DIAZ-MONTES, T. P., BRISTOW, R. E., & OELKE, M. (2009). Ovarian Cancer-associated Ascites Demonstrates Altered Immune Environment: Implications for Antitumor Immunity. *Anticancer Research, 29*(8), 2875-2884.

Green, D. S., Husain, S. R., Johnson, C. L., Sato, Y., Han, J., Joshi, B., . . . Zoon, K. C. (2019). Combination immunotherapy with IL-4 Pseudomonas exotoxin and IFN-α and IFN-γ mediate antitumor effects in vitro and in a mouse model of human ovarian cancer. *Immunotherapy, 11*(6), 483-496. doi:10.2217/imt-2018-0158

Guan, Y., Chen, X., Wu, M., Zhu, W., Arslan, A., Takeda, S., . . . Peltz, G. (2020). The phosphatidylethanolamine biosynthesis pathway provides a new target for cancer chemotherapy. *Journal of Hepatology, 72*(4), 746-760. doi:10.1016/j.jhep.2019.11.007

Hamanishi, J., Mandai, M., Abiko, K., Matsumura, N., Baba, T., Yoshioka, Y., . . . Konishi, I. (2011). The comprehensive assessment of local immune status of ovarian cancer by the clustering of multiple immune factors. *Clin Immunol, 141*(3), 338-347. doi:10.1016/j.clim.2011.08.013

He, D., Li, H., Yusuf, N., Elmets, C. A., Li, J., Mountz, J. D., & Xu, H. (2010). IL-17 Promotes Tumor Development through the Induction of Tumor Promoting Microenvironments at Tumor Sites and Myeloid-Derived Suppressor Cells. *The Journal of Immunology, 184*(5), 2281-2288.

Herzog, T. J. (2004). Recurrent ovarian cancer: how important is it to treat to disease progression? *Clin Cancer Res, 10*(22), 7439-7449. doi:10.1158/1078-0432.Ccr-04-0683

Hume, D. A., Radik, J. L., Ferber, E., & Weidemann, M. J. (1978). Aerobic glycolysis and lymphocyte transformation. *Biochemical Journal, 174*(3), 703-709. doi:10.1042/bj1740703

Hwang, W. T., Adams, S. F., Tahirovic, E., Hagemann, I. S., & Coukos, G. (2012). Prognostic significance of tumor-infiltrating T cells in ovarian cancer: a meta-analysis. *Gynecologic Oncology 124*(2), 192-198. doi:10.1016/j.ygyno.2011.09.039

Icard, P., Alifano, M., Donnadieu, E., & Simula, L. (2021). Fructose-1,6-bisphosphate promotes PI3K and glycolysis in T cells? *Trends in Endocrinology and Metabolism, 32*(8), 540-543. doi:10.1016/j.tem.2021.04.013

Icard, P., Shulman, S., Farhat, D., Steyaert, J. M., Alifano, M., & Lincet, H. (2018). How the Warburg effect supports aggressiveness and drug resistance of cancer cells? *Drug Resist Updat, 38*, 1-11. doi:10.1016/j.drup.2018.03.001

Jang, M., Kim, S. S., & Lee, J. (2013). Cancer cell metabolism: implications for therapeutic targets. *Experimental and Molecular Medicine, 45*(10), e45. doi:10.1038/emm.2013.85

Jiang, Y. X., Siu, M. K. Y., Wang, J. J., Leung, T. H. Y., Chan, D. W., Cheung, A. N. Y., . . . Chan, K. K. L. (2022). PFKFB3 Regulates Chemoresistance, Metastasis and Stemness via IAP Proteins and the NF-κB Signaling Pathway in Ovarian Cancer. *Frontiers in Oncology, 12*, 748403. doi:10.3389/fonc.2022.748403

Kaku, T., Ogawa, S., Kawano, Y., Ohishi, Y., Kobayashi, H., Hirakawa, T., & Nakano, H. (2003). Histological classification of ovarian cancer. *Medical Electron Microscopy, 36*(1), 9-17.

Kampan, N. C., Madondo, M. T., Reynolds, J., Hallo, J., McNally, O. M., Jobling, T. W., . . . Plebanski, M. (2020). Pre-operative sera interleukin-6 in the diagnosis of high-grade serous ovarian cancer. *Scientific Reports, 10*(1), 2213. doi:10.1038/s41598-020-59009-z

Karthikeyan, S., Geschwind, J. F., & Ganapathy-Kanniappan, S. (2014). Tumor cells and memory T cells converge at glycolysis: therapeutic implications. *Cancer Biology and Therapy, 15*(5), 483-485. doi:10.4161/cbt.28160

Khazaei, Z., Namayandeh, S. M., Beiranvand, R., Naemi, H., Bechashk, S. M., & Goodarzi, E. (2021). Worldwide incidence and mortality of ovarian cancer and Human Development Index (HDI): GLOBOCAN sources and methods 2018. *Journal of Preventive Medicine and Hygiene, 62*(1), E174-184. doi:10.15167/2421-4248/jpmh2021.62.1.1606

Kim, S., Kim, B., & Song, Y. S. (2016). Ascites modulates cancer cell behavior, contributing to tumor heterogeneity in ovarian cancer. *Cancer Science, 107*(9), 1173-1178. doi:10.1111/cas.12987

Kioi, M., Takahashi, S., Kawakami, M., Kawakami, K., Kreitman, R. J., & Puri, R. K. (2005). Expression and targeting of interleukin-4 receptor for primary and advanced ovarian cancer therapy. *Cancer Research, 65*(18), 8388-8396. doi:10.1158/0008-5472.Can-05-1043

Kishton, R. J., Barnes, C. E., Nichols, A. G., Cohen, S., Gerriets, V. A., Siska, P. J., . . . Rathmell, J. C. (2016). AMPK Is Essential to Balance Glycolysis and Mitochondrial Metabolism to Control T-ALL Cell Stress and Survival. *Cell Metabolism, 23*(4), 649-662. doi:10.1016/j.cmet.2016.03.008

Knutson, K. L., Almand, B., Dang, Y., & Disis, M. L. (2004). Neu antigen-negative variants can be generated after neu-specific antibody therapy in neu transgenic mice. *Cancer Research, 64*(3), 1146-1151. doi:10.1158/0008-5472.can-03-0173

Kocemba, K. A., DuljDska-Litewka, J., WojdyBa, K. L., & Q kala, P. A. (2016). The role of 6-phosphofructo-2-kinase (PFK-2)/fructose 2,6-bisphosphatase (FBPase-2) in metabolic reprogramming of cancer cells. *Postepy higieny i medycyny doswiadczalnej, 70 0*, 938-950.

Kossaï, M., Leary, A., Scoazec, J. Y., & Genestie, C. (2018). Ovarian Cancer: A Heterogeneous Disease. *Pathobiology, 85*(1-2), 41-49. doi:10.1159/000479006

Krauss, S., Brand, M. D., & Buttgereit, F. (2001). Signaling takes a breath--new quantitative perspectives on bioenergetics and signal transduction. *Immunity, 15*(4), 497-502. doi:10.1016/s1074-7613(01)00205-9

Lai, Y.-P., Jeng, C.-J., & Chen, S.-C. (2011). The roles of CD4+ T cells in tumor immunity. *ISRN Immunology, 2011*, 1-6.

Lambeck, A. J., Crijns, A. P., Leffers, N., Sluiter, W. J., ten Hoor, K. A., Braid, M., . . . Kast, W. M. (2007). Serum cytokine profiling as a diagnostic and prognostic tool in ovarian cancer: a potential role for interleukin 7. *Clinical Cancer Research, 13*(8), 2385-2391. doi:10.1158/1078-0432.Ccr-06-1828

Le, A., Cooper, C. R., Gouw, A. M., Dinavahi, R., Maitra, A., Deck, L. M., . . . Dang, C. V. (2010). Inhibition of lactate dehydrogenase A induces oxidative stress and inhibits tumor progression. *Proceedings of the National Academy of Sciences of the United States of America, 107*(5), 2037-2042. doi:10.1073/pnas.0914433107

Li, A. J., & Karlan, B. Y. (2003). Surgical advances in the treatment of ovarian cancer. *Hematol Oncol Clin North Am, 17*(4), 945-956. doi:10.1016/s0889-8588(03)00062-5

Li, J., Wang, J., Chen, R., Bai, Y., & Lu, X. (2017). The prognostic value of tumor-infiltrating T lymphocytes in ovarian cancer. *Oncotarget, 8*(9), 15621-15631. doi:10.18632/oncotarget.14919

Li, W., Qu, G., Choi, S. C., Cornaby, C., Titov, A., Kanda, N., . . . Morel, L. (2019). Targeting T Cell Activation and Lupus Autoimmune Phenotypes by Inhibiting Glucose Transporters. *Frontiers in Immunology, 10*, 833. doi:10.3389/fimmu.2019.00833

Li, X., Liu, J., Qian, L., Ke, H., Yao, C., Tian, W., . . . Zhang, J. (2018). Expression of PFKFB3 and Ki67 in lung adenocarcinomas and targeting PFKFB3 as a therapeutic strategy. *Mol Cell Biochem, 445*(1-2), 123-134. doi:10.1007/s11010-017-3258-8

Lu, L., Chen, Y., & Zhu, Y. (2017). The molecular basis of targeting PFKFB3 as a therapeutic strategy against cancer. *Oncotarget, 8*(37), 62793-62802. doi:10.18632/oncotarget.19513

Luby, A., & Alves-Guerra, M. C. (2021). Targeting Metabolism to Control Immune Responses in Cancer and Improve Checkpoint Blockade Immunotherapy. *Cancers (Basel), 13*(23). doi:10.3390/cancers13235912

Luo, J. H., Zhang, C. Y., Lu, C. Y., Guo, G. H., Tian, Y. P., & Li, Y. L. (2017). Serum expression level of cytokine and chemokine correlates with progression of human ovarian cancer. *European Journal of Gynaecological Oncology, 38*(1), 33-39.

Luo, X., Xu, J., Yu, J., & Yi, P. (2021). Shaping Immune Responses in the Tumor Microenvironment of Ovarian Cancer. *Frontiers in Immunology, 12*. doi:10.3389/fimmu.2021.692360

Ma, Y., Wang, W., Idowu, M. O., Oh, U., Wang, X. Y., Temkin, S. M., & Fang, X. (2018). Ovarian Cancer Relies on Glucose Transporter 1 to Fuel Glycolysis and Growth: Anti-Tumor Activity of BAY-876. *Cancers (Basel), 11*(1). doi:10.3390/cancers11010033

Mabuchi, S., Kuroda, H., Takahashi, R., & Sasano, T. (2015). The PI3K/AKT/mTOR pathway as a therapeutic target in ovarian cancer. *Gynecologic Oncology, 137*(1), 173-179. doi:10.1016/j.ygyno.2015.02.003

Malekzadeh, M., Dehaghani, A. S., Ghaderi, A., & Doroudchi, M. (2013). IL-17A is elevated in sera of patients with poorly differentiated ovarian papillary serous cystadenocarcinoma. *Cancer Biomarkers, 13*(6), 417-425. doi:10.3233/cbm-140392

Marchetti, C., De Felice, F., Perniola, G., Palaia, I., Musella, A., Di Donato, V., . . . Benedetti Panici, P. (2019). Role of intraperitoneal chemotherapy in ovarian cancer in the platinum-taxane-based era: A meta-analysis. *Critical Reviews in Oncology and Hematology, 136*, 64-69. doi:10.1016/j.critrevonc.2019.01.002

Marth, C., Zeimet, A. G., Herold, M., Brumm, C., Windbichler, G., Müller-Holzner, E., . . . Daxenbichler, G. (1996). Different effects of interferons, interleukin-1beta and tumor necrosis factor-alpha in normal (OSE) and malignant human ovarian epithelial cells. *International Journal of Cancer, 67*(6), 826-830. doi:10.1002/(sici)1097-0215(19960917)67:6<826::Aid-ijc12>3.0.Co;2-#

Martins, C. P., New, L. A., O'Connor, E. C., Previte, D. M., Cargill, K. R., Tse, I. L., . . . Piganelli, J. D. (2021). Glycolysis Inhibition Induces Functional and Metabolic Exhaustion of CD4(+) T Cells in Type 1 Diabetes. *Frontiers in Immunology, 12*, 669456. doi:10.3389/fimmu.2021.669456

Matsumoto, K., Noda, T., Kobayashi, S., Sakano, Y., Yokota, Y., Iwagami, Y., . . . Eguchi, H. (2021). Inhibition of glycolytic activator PFKFB3 suppresses tumor growth and induces tumor vessel normalization in hepatocellular carcinoma. *Cancer Letters, 500*, 29-40. doi:10.1016/j.canlet.2020.12.011

McCloskey, C. W., Goldberg, R. L., Carter, L. E., Gamwell, L. F., Al-Hujaily, E. M., Collins, O., . . . Vanderhyden, B. C. (2014). A new spontaneously transformed syngeneic model of high-grade serous ovarian cancer with a tumor-initiating cell population. *Frontiers in Oncology, 4*, Article 53. doi:10.3389/fonc.2014.00053

Michalek, R. D., Gerriets, V. A., Jacobs, S. R., Macintyre, A. N., MacIver, N. J., Mason, E. F., . . . Rathmell, J. C. (2011). Cutting edge: distinct glycolytic and lipid oxidative metabolic programs are essential for effector and regulatory CD4+ T cell subsets. *The Journal of Immunology, 186*(6), 3299-3303. doi:10.4049/jimmunol.1003613

Mondal, S., Roy, D., Camacho-Pereira, J., Khurana, A., Chini, E., Yang, L., . . . Shridhar, V. (2015). HSulf-1 deficiency dictates a metabolic reprograming of

glycolysis and TCA cycle in ovarian cancer. *Oncotarget, 6*(32), 33705-33719. doi:10.18632/oncotarget.5605

Mondal, S., Roy, D., Sarkar Bhattacharya, S., Jin, L., Jung, D., Zhang, S., . . . Shridhar, V. (2019). Therapeutic targeting of PFKFB3 with a novel glycolytic inhibitor PFK158 promotes lipophagy and chemosensitivity in gynecologic cancers. *International Journal of Cancer, 144*(1), 178-189. doi:10.1002/ijc.31868

Mosmann, T. (1983). Rapid colorimetric assay for cellular growth and survival: application to proliferation and cytotoxicity assays. *Journal of Immunological Methods, 65*(1-2), 55-63. doi:10.1016/0022-1759(83)90303-4

National Library of Medicine (NCT02044861). (January 2014 -). Phase 1 Safety Study of ACT-PFK-158, 2HCl in Patients With Advanced Solid Malignancies. In.

Niu, N., Yao, J., Bast, R. C., Sood, A. K., & Liu, J. (2021). IL-6 promotes drug resistance through formation of polyploid giant cancer cells and stromal fibroblast reprogramming. *Oncogenesis, 10*(9), 65. doi:10.1038/s41389-021-00349-4

O'Donnell, J. S., Teng, M. W. L., & Smyth, M. J. (2019). Cancer immunoediting and resistance to T cell-based immunotherapy. *Nature Reviews. Clinical Oncology, 16*(3), 151-167. doi:10.1038/s41571-018-0142-8

Odunsi, K. (2017). Immunotherapy in ovarian cancer. *Annals of Oncology - official journal of the European Society for medical oncology, 28*(supplement nr. 8), VIII1-VIII7. doi:10.1093/annonc/mdx444

Palmer, C. S., Ostrowski, M., Balderson, B., Christian, N., & Crowe, S. M. (2015). Glucose metabolism regulates T cell activation, differentiation, and functions. *Frontiers in Immunology, 6*, 1. doi:10.3389/fimmu.2015.00001

Park, J. H., Pyun, W. Y., & Park, H. W. (2020). Cancer Metabolism: Phenotype, Signaling and Therapeutic Targets. *Cells, 9*(10). doi:10.3390/cells9102308

Pearce, E. L. (2010). Metabolism in T cell activation and differentiation. *Current Opinion in Immunology, 22*(3), 314-320. doi:10.1016/j.coi.2010.01.018

Pereira, J., Romao, V., Eulálio, M., Jorge, R., Breda, F., Calretas, S., . . . Carvalho, A. (2015). Sclerosing Mesenteritis and Disturbance of Glucose Metabolism: A New Relationship? A Case Series. *American Journal of Case Reports 16*. doi:10.12659/AJCR.896145

Pignata, S., Cannella, L., Leopardo, D., Pisano, C., Bruni, G. S., & Facchini, G. (2011). Chemotherapy in epithelial ovarian cancer. *Cancer Letters, 303*(2), 73-83. doi:10.1016/j.canlet.2011.01.026

Pouessel, D., Culine, S., Guillot, A., Di Stabile, L., Thibaudeau, E., Reymond, D., & Mottet, N. (2008). *Phase II Study of TLN-232*, a novel M2PK targeting agent, administered by CIV to patients with advanced renal cell carcinoma (RCC)* Paper presented at the ANNALS OF ONCOLOGY.

Rabinovich, A., Medina, L., Piura, B., & Huleihel, M. (2010). Expression of IL-10 in human normal and cancerous ovarian tissues and cells. *European Cytokine Network, 21*(2), 122-128. doi:10.1684/ecn.2010.0188

Raskov, H., Orhan, A., Christensen, J. P., & Gögenur, I. (2021). Cytotoxic CD8+ T cells in cancer and cancer immunotherapy. *British Journal of Cancer, 124*(2), 359-367. doi:10.1038/s41416-020-01048-4

Ray, U., Roy, D., Jin, L., Thirusangu, P., Staub, J., Xiao, Y., . . . Shridhar, V. (2021). Group III phospholipase A2 downregulation attenuated survival and metastasis in ovarian cancer and promotes chemo-sensitization. *Journal of Experimental Clinical Cancer Research, 40*(1), 182. doi:10.1186/s13046-021-01985-9

Renner, K., Bruss, C., Schnell, A., Koehl, G., Becker, H. M., Fante, M., . . . Kreutz, M. (2019). Restricting Glycolysis Preserves T Cell Effector Functions and Augments Checkpoint Therapy. *Cell Reports, 29*(1), 135-150.

Renner, K., Geiselhöringer, A. L., Fante, M., Bruss, C., Färber, S., Schönhammer, G., . . . Kreutz, M. (2015). Metabolic plasticity of human T cells: Preserved cytokine production under glucose deprivation or mitochondrial restriction, but 2-deoxy-glucose affects effector functions. *European Journal of Immunology, 45*(9), 2504-2516. doi:10.1002/eji.201545473

Reutter, M., Emons, G., & Gründker, C. (2013). Starving tumors: inhibition of glycolysis reduces viability of human endometrial and ovarian cancer cells and enhances antitumor efficacy of GnRH receptor-targeted therapies. *Int J Gynecol Cancer, 23*(1), 34-40. doi:10.1097/IGC.0b013e318275b028

Rogala, E., Nowicka, A., Wertel, I., Polak, G., Tarkowski, R., Kotarski, J., & Kotarski, J. (2011). Th17 lymphocytes - a new ally in the fight against ovarian cancer? *Postepy Biologii Komorki, 38*, 423-433.

Romero, I., Leskelä, S., Mies, B. P., Velasco, A. P., & Palacios, J. (2020). Morphological and molecular heterogeneity of epithelial ovarian cancer: Therapeutic implications. *European Journal of Cancer Supplements, 15*, 1-15.

Rossi, J. F., Lu, Z. Y., Jourdan, M., & Klein, B. (2015). Interleukin-6 as a therapeutic target. *Clinical Cancer Research, 21*(6), 1248-1257. doi:10.1158/1078-0432.Ccr-14-2291

Salerno, F., Guislain, A., Cansever, D., & Wolkers, M. C. (2016). TLR-Mediated Innate Production of IFN-γ by CD8+ T Cells Is Independent of Glycolysis. *The Journal of Immunology, 196*(9), 3695-3705. doi:10.4049/jimmunol.1501997

Sanguinete, M. M. M., Oliveira, P. H., Martins-Filho, A., Micheli, D. C., Tavares-Murta, B. M., Murta, E. F. C., & Nomelini, R. S. (2017). Serum IL-6 and IL-8 Correlate with Prognostic Factors in Ovarian Cancer. *Immunological Investigations, 46*(7), 677-688. doi:10.1080/08820139.2017.1360342

Santoiemma, P. P., & Powell, D. J., Jr. (2015). Tumor infiltrating lymphocytes in ovarian cancer. *Cancer Biology and Therapy, 16*(6), 807-820. doi:10.1080/15384047.2015.1040960

Sarkar Bhattacharya, S., Thirusangu, P., Jin, L., Roy, D., Jung, D., Xiao, Y., . . . Shridhar, V. (2019). PFKFB3 inhibition reprograms malignant pleural mesothelioma to nutrient stress-induced macropinocytosis and ER stress as independent binary adaptive responses. *Cell Death & Disease, 10*(10), 725.

Sato, E., Olson, S. H., Ahn, J., Bundy, B., Nishikawa, H., Qian, F., . . . Odunsi, K. (2005). Intraepithelial CD8+ tumor-infiltrating lymphocytes and a high CD8+/regulatory T cell ratio are associated with favorable prognosis in ovarian cancer. *Proceedings of the National Academy of Sciences of the United States of America, 102*(51), 18538-18543. doi:10.1073/pnas.0509182102

Scambia, G., Testa, U., Benedetti Panici, P., Foti, E., Martucci, R., Gadducci, A., . . . Mancuso, S. (1995). Prognostic significance of interleukin 6 serum levels in patients with ovarian cancer. *British Journal of Cancer, 71*(2), 354-356. doi:10.1038/bjc.1995.71

Schauer, I. G., Zhang, J., Xing, Z., Guo, X., Mercado-Uribe, I., Sood, A. K., . . . Liu, J. (2013). Interleukin-1β promotes ovarian tumorigenesis through a p53/NF-κB-mediated inflammatory response in stromal fibroblasts. *Neoplasia, 15*(4), 409-420. doi:10.1593/neo.121228

Schröder, W., Ruppert, C., & Bender, H. G. (1994). Concomitant measurements of interleukin-6 (IL-6) in serum and peritoneal fluid of patients with benign and malignant ovarian tumors. *European Journal of Obstetrics, Gynecology and Reproductive Biology, 56*(1), 43-46. doi:10.1016/0028-2243(94)90152-x

Sen, S., Kuru, O., Akbayır, O., Oğuz, H., Yasasever, V., & Berkman, S. (2011). Determination of serum CRP, VEGF, Leptin, CK-MB, CA-15-3 and IL-6 levels for malignancy prediction in adnexal masses. *Journl of the Turkish German Gynecological Association, 12*(4), 214-219. doi:10.5152/jtgga.2011.54

Shen, H., & Shi, L. Z. (2019). Metabolic regulation of T(H)17 cells. *Molecular Immunology, 109*, 81-87. doi:10.1016/j.molimm.2019.03.005

Shi, L. Z., Wang, R., Huang, G., Vogel, P., Neale, G., Green, D. R., & Chi, H. (2011). HIF1alpha-dependent glycolytic pathway orchestrates a metabolic checkpoint for the differentiation of TH17 and Treg cells. *The Journal of Experimental Medicine, 208*(7), 1367-1376. doi:10.1084/jem.20110278

Simon-Molas, H., Arnedo-Pac, C., Fontova, P., Vidal-Alabró, A., Castaño, E., Rodríguez-García, A., . . . Bartrons, R. (2018). PI3K-Akt signaling controls PFKFB3 expression during human T-lymphocyte activation. *Molecular and Cellular Biochemistry, 448*(1-2), 187-197. doi:10.1007/s11010-018-3325-9

Spear, P., Barber, A., Rynda-Apple, A., & Sentman, C. L. (2012). Chimeric antigen receptor T cells shape myeloid cell function within the tumor microenvironment through IFN-γ and GM-CSF. *Journal of Immunology, 188*(12), 6389-6398. doi:10.4049/jimmunol.1103019

Stadlmann, S., Amberger, A., Pollheimer, J., Gastl, G., Offner, F., Margreiter, R., & Zeimet, A. (2005). Ovarian carcinoma cells and IL-1 beta-activated human peritoneal mesothelial cells are possible sources of vascular endothelial growth factor in inflammatory and malignant peritoneal effusions. *Gynecologic Oncology, 97*, 784-789. doi:10.1016/j.gygno.2005.02.017

Sukumar, M., Liu, J., Ji, Y., Subramanian, M., Crompton, J. G., Yu, Z., . . . Gattinoni, L. (2013). Inhibiting glycolytic metabolism enhances CD8+ T cell memory and antitumor function. *The Journal of Clinical Investigation, 123*(10), 4479-4488. doi:10.1172/jci69589

Sun, L., Kees, T., Almeida, A. S., Liu, B., He, X. Y., Ng, D., . . . Egeblad, M. (2021). Activating a collaborative innate-adaptive immune response to control metastasis. *Cancer Cell, 39*(10), 1361-1374. doi:10.1016/j.ccell.2021.08.005

Sung, H., Ferlay, J., Siegel, R. L., Laversanne, M., Soerjomataram, I., Jemal, A., & Bray, F. (2021). Global cancer statistics 2020: GLOBOCAN estimates of incidence and mortality worldwide for 36 cancers in 185 countries. *CA: a cancer journal for clinicians, 71*(3), 209-249.

Szulc-Kielbik, I., Kielbik, M., Nowak, M., & Klink, M. (2021). The implication of IL-6 in the invasiveness and chemoresistance of ovarian cancer cells. Systematic review of its potential role as a biomarker in ovarian cancer patients. *Biochimica et Biophysica Acta (BBA) - Reviews on Cancer, 1876*(2), 188639. doi:https://doi.org/10.1016/j.bbcan.2021.188639

Tang, R., Xu, J., Zhang, B., Liu, J., Liang, C., Hua, J., . . . Shi, S. (2020). Ferroptosis, necroptosis, and pyroptosis in anticancer immunity. *Journal of Hematology and Oncology, 13*(1), 110. doi:10.1186/s13045-020-00946-7

Telang, S., Clem, B. F., Klarer, A. C., Clem, A. L., Trent, J. O., Bucala, R., & Chesney, J. (2012). Small molecule inhibition of 6-phosphofructo-2-kinase suppresses t cell activation. *Journal of Translational Medicine, 10*, 95. doi:10.1186/1479-5876-10-95

Tempfer, C., Zeisler, H., Sliutz, G., Haeusler, G., Hanzal, E., & Kainz, C. (1997). Serum evaluation of interleukin 6 in ovarian cancer patients. *Gynecologic Oncology, 66*(1), 27-30. doi:10.1006/gyno.1997.4726

Todaro, M., Lombardo, Y., Francipane, M. G., Alea, M. P., Cammareri, P., Iovino, F., . . . Stassi, G. (2008). Apoptosis resistance in epithelial tumors is mediated by tumor-cell-derived interleukin-4. *Cell Death and Differentiation, 15*(4), 762-772. doi:10.1038/sj.cdd.4402305

Tomsová, M., Melichar, B., Sedláková, I., & Steiner, I. (2008). Prognostic significance of CD3+ tumor-infiltrating lymphocytes in ovarian carcinoma. *Gynecol Oncol, 108*(2), 415-420. doi:10.1016/j.ygyno.2007.10.016

Torre, L. A., Trabert, B., DeSantis, C. E., Miller, K. D., Samimi, G., Runowicz, C. D., . . . Siegel, R. L. (2018). Ovarian cancer statistics, 2018. *CA: a cancer journal for clinicians, 68*(4), 284-296.

Vander Heiden, M. G., Cantley, L. C., & Thompson, C. B. (2009). Understanding the Warburg effect: the metabolic requirements of cell proliferation. *Science, 324*(5930), 1029-1033. doi:10.1126/science.1160809

Wall, L., Burke, F., Barton, C., Smyth, J., & Balkwill, F. (2003). IFN-gamma induces apoptosis in ovarian cancer cells in vivo and in vitro. *Clinical Cancer Research, 9*(7), 2487-2496.

Wang, H., & Ye, J. (2015). Regulation of energy balance by inflammation: common theme in physiology and pathology. *Reviews in Endocrine and Metabolic Disorders, 16*(1), 47-54. doi:10.1007/s11154-014-9306-8

Wang, R. F. (2001). The role of MHC class II-restricted tumor antigens and CD4+ T cells in antitumor immunity. *Trends in Immunology, 22*(5), 269-276. doi:10.1016/s1471-4906(01)01896-8

Wang, T., Marquardt, C., & Foker, J. (1976). Aerobic glycolysis during lymphocyte proliferation. *Nature, 261*(5562), 702-705.

Wang, W., Zou, W., & Liu, J. R. (2018). Tumor-infiltrating T cells in epithelial ovarian cancer: predictors of prognosis and biological basis of immunotherapy. *Gynecologic Oncology, 151*(1), 1-3. doi:10.1016/j.ygyno.2018.09.005

Wang, Y., Yang, J., Gao, Y., Du, Y., Bao, L., Niu, W., & Yao, Z. (2005). Regulatory effect of e2, IL-6 and IL-8 on the growth of epithelial ovarian cancer cells. *Cellular and Molecular Immunology, 2*(5), 365-372.

Warburg, O. (1956). On respiratory impairment in cancer cells. *Science, 124*(3215), 269-270.

Warburg, O., Wind, F., & Negelein, E. (1927). THE METABOLISM OF TUMORS IN THE BODY. *The Journal of General Physiology, 8*(6), 519-530. doi:10.1085/jgp.8.6.519

Ward, P. S., & Thompson, C. B. (2012). Metabolic reprogramming: a cancer hallmark even warburg did not anticipate. *Cancer Cell, 21*(3), 297-308. doi:10.1016/j.ccr.2012.02.014

Watanabe, T., Hashimoto, T., Sugino, T., Soeda, S., Nishiyama, H., Morimura, Y., . . . Fujimori, K. (2012). Production of IL1-beta by ovarian cancer cells induces mesothelial cell beta1-integrin expression facilitating peritoneal dissemination. *Journal of Ovarian Research, 5*(1), 7. doi:10.1186/1757-2215-5-7

Wefers, C., Duiveman-de Boer, T., Yigit, R., Zusterzeel, P. L. M., van Altena, A. M., Massuger, L., & De Vries, I. J. M. (2018). Survival of Ovarian Cancer Patients Is Independent of the Presence of DC and T Cell Subsets in Ascites. *Frontiers in Immunology, 9*, 3156. doi:10.3389/fimmu.2018.03156

Wieder, T., Braumüller, H., Kneilling, M., Pichler, B., & Röcken, M. (2008). T cell-mediated help against tumors. *Cell Cycle, 7*(19), 2974-2977. doi:10.4161/cc.7.19.6798

Wilke, C. M., Kryczek, I., Wei, S., Zhao, E., Wu, K., Wang, G., & Zou, W. (2011). Th17 cells in cancer: help or hindrance? *Carcinogenesis, 32*(5), 643-649. doi:10.1093/carcin/bgr019

Wong, J. Y., Huggins, G. S., Debidda, M., Munshi, N. C., & De Vivo, I. (2008). Dichloroacetate induces apoptosis in endometrial cancer cells. *Gynecologic Oncology, 109*(3), 394-402. doi:10.1016/j.ygyno.2008.01.038

Woolery, K. T., Mohamed, M., Linger, R. J., Dobrinski, K. P., Roman, J., & Kruk, P. A. (2015). BRCA1 185delAG Mutation Enhances Interleukin-1β Expression in Ovarian Surface Epithelial Cells. *Biomed Research International, 2015*, 652017. doi:10.1155/2015/652017

Xiao, Y., Jin, L., Deng, C., Guan, Y., Kalogera, E., Ray, U., . . . Shridhar, V. (2021). Inhibition of PFKFB3 induces cell death and synergistically enhances chemosensitivity in endometrial cancer. *Oncogene, 40*(8), 1409-1424. doi:10.1038/s41388-020-01621-4

Xintaropoulou, C., Ward, C., Wise, A., Marston, H., Turnbull, A., & Langdon, S. P. (2015). A comparative analysis of inhibitors of the glycolysis pathway in breast and ovarian cancer cell line models. *Oncotarget, 6*(28), 25677-22695. doi:10.18632/oncotarget.4499

Xintaropoulou, C., Ward, C., Wise, A., Queckborner, S., Turnbull, A., Michie, C. O., . . . Langdon, S. P. (2018). Expression of glycolytic enzymes in ovarian cancers and evaluation of the glycolytic pathway as a strategy for ovarian cancer treatment. *BMC Cancer, 18*(1), 636. doi:10.1186/s12885-018-4521-4

Yalcin, A., Clem, B. F., Simmons, A., Lane, A., Nelson, K., Clem, A. L., . . . Chesney, J. (2009). Nuclear targeting of 6-phosphofructo-2-kinase (PFKFB3) increases

proliferation via cyclin-dependent kinases. *The Journal of Biological Chemistry, 284*(36), 24223-24232. doi:10.1074/jbc.M109.016816

Yalcin, A., Telang, S., Clem, B., & Chesney, J. (2009). Regulation of glucose metabolism by 6-phosphofructo-2-kinase/fructose-2,6-bisphosphatases in cancer. *Exp Mol Pathol, 86*(3), 174-179. doi:10.1016/j.yexmp.2009.01.003

Yang, Z., Goronzy, J. J., & Weyand, C. M. (2014). The glycolytic enzyme PFKFB3/phosphofructokinase regulates autophagy. *Autophagy, 10*(2), 382-383. doi:10.4161/auto.27345

Yao, F., Yan, S., Wang, X., Shi, D., Bai, J., Li, F., . . . Qian, B. (2014). Role of IL-17F T7488C polymorphism in carcinogenesis: a meta-analysis. *Tumour Biology, 35*(9), 9061-9068. doi:10.1007/s13277-014-2171-y

Ye, J., Su, X., Hsueh, E. C., Zhang, Y., Koenig, J. M., Hoft, D. F., & Peng, G. (2011). Human tumor-infiltrating Th17 cells have the capacity to differentiate into IFN-γ+ and FOXP3+ T cells with potent suppressive function. *European Journal of Immunology, 41*(4), 936-951. doi:10.1002/eji.201040682

Yousefi, H., Momeny, M., Ghaffari, S. H., Parsanejad, N., Poursheikhani, A., Javadikooshesh, S., . . . Ghavamzadeh, A. (2018). IL-6/IL-6R pathway is a therapeutic target in chemoresistant ovarian cancer. *Tumori Journal, 105*(1), 84-91. doi:10.1177/0300891618784790

Zentrum für Krebsregisterdaten. (2021). Eierstockkrebs (Ovarialkarzinom). Retrieved from https://www.krebsdaten.de/Krebs/DE/Content/Krebsarten/Eierstockkrebs/eierstockkrebs_node.html

Zhang, J., Xue, W., Xu, K., Yi, L., Guo, Y., Xie, T., . . . Zhang, W. (2020). Dual inhibition of PFKFB3 and VEGF normalizes tumor vasculature, reduces lactate production, and improves chemotherapy in glioblastoma: insights from protein expression profiling and MRI. *Theranostics, 10*(16), 7245-7259. doi:10.7150/thno.44427

Zhang, L., Conejo-Garcia, J. R., Katsaros, D., Gimotty, P. A., Massobrio, M., Regnani, G., . . . Coukos, G. (2003). Intratumoral T cells, recurrence, and survival in epithelial ovarian cancer. *The New England Journal of Medicine, 348*(3), 203-213. doi:10.1056/NEJMoa020177

Zhang, L., Liu, W., Wang, X., Wang, X., & Sun, H. (2019). Prognostic value of serum IL-8 and IL-10 in patients with ovarian cancer undergoing chemotherapy. *Oncology Letters, 17*(2), 2365-2369. doi:10.3892/ol.2018.9842

Zhang, R., Roque, D. M., Reader, J., & Lin, J. (2022). Combined inhibition of IL-6 and IL-8 pathways suppresses ovarian cancer cell viability and migration and tumor growth. *International Journal of Oncology, 60*(5). doi:10.3892/ijo.2022.5340

Zhang, X., Weng, W., Xu, W., Wang, Y., Yu, W., Tang, X., . . . Sun, F. (2014). Prognostic significance of interleukin 17 in cancer: a meta-analysis. *International Journal of Clinical and Experimental Medicine, 7*(10), 3258-3269.

Zhao, Y., Butler, E. B., & Tan, M. (2013). Targeting cellular metabolism to improve cancer therapeutics. *Cell Death Dis, 4*(3), e532.

Zheng, Y., Delgoffe, G. M., Meyer, C. F., Chan, W., & Powell, J. D. (2009). Anergic T cells are metabolically anergic. *Journal of Immunology, 183*(10), 6095-6101. doi:10.4049/jimmunol.0803510

Zhou, F. (2009). Molecular mechanisms of IFN-gamma to up-regulate MHC class I antigen processing and presentation. *International Reviews of Immunology, 28*(3-4), 239-260. doi:10.1080/08830180902978120

Zhu, X., Ying, L. S., Xu, S. H., Zhu, C. H., & Xie, J. B. (2010). [Clinicopathologic and prognostic significance of serum levels of cytokines in patients with advanced serous ovarian cancer prior to surgery]. *Zhonghua Bing Li Xue Za Zhi, 39*(10), 666-670.

XI. Acknowledgements

This work was conducted under the supervision and support of the Mayo Clinic division of experimental pathology and laboratory medicine under Dr. Vijayalakshmi Shridhar.

I would like to express my deepest gratitude to Vijayalakshmi Shridhar, Ph.D. for the extraordinary opportunity to work under her guidance at the Mayo Clinic, Rochester Minnesota and Matt Block, M.D., Ph.D. for kindness, excellent advice and the encouragement to pursue the unknown.

My sincere and cordial thanks to Prof. Dr. med. Ralf Schmidmaier, for his exceptional support at the Ludwig-Maximillians-University, Munich.

My special thanks to Dr. Debarshi Roy for his invaluable patience and feedback, words of motivation and expert teaching sessions.

Additionally, I would also like to acknowledge Robert Hoffmann, M.D. for paving the way for German students in Rochester and setting an inspiring example of hard work and dedication.

I would like to extend my sincere gratitude to Julie Staub and Courtney Erskine for generously providing knowledge and valuable hands-on method assistance.

Many thanks to my friends and colleagues, who made the time in Rochester a truly unique end unforgettable experience.

Most importantly, I am grateful for my mother's unconditional, unequivocal and loving support throughout the entire thesis process. My accomplishments are because she always believed in me.

Finally, I owe my deepest gratitude to Samuel, who is my love.

XII. Supplementary information

Mouse autopsy; histopathological report from 20th of February, 2018 (Representative for PFK-158 treatment group).

IDEXX BioResearch

FINAL REPORT OF LABORATORY EXAMINATION
4011 Discovery Drive, Columbia, MO 65201
1-800-669-0825 1-573-499-5700
idexxbioresearch@idexx.com www.idexxbioresearch.com

IDEXX BioResearch Case # 5899-2018

Received: 2/15/2018
Completed: 2/20/2018

Submitted By

Thomas Meier
Mayo Clinic
200 First St SW
Rochester, MN 55905

Phone: 507-284-1050
Email: meier.thomas@mayo.edu; vettechs@mayo.edu

Specimen Description

Species: mouse
Description: Fixed tissues
Number of Specimens/Animals: 1
Building/Facility: Guggenheim

Purchase Order #: 65654039

Client ID	Investigator	Strain /Breed	Sex	Age
1	Shridhar	FVB	F	Adult

Services/Tests Performed: Histopathology Services

Histopathologic evaluation for: cecum, colon, duodenum, jejunum, kidney, liver, mesentery, pancreas, stomach

General Comments: See submitted gross necropsy report by Katie LaVallee; tissues submitted: gastrointestinal tract, left kidney, liver.Note: we were unsure which histology panel to select. Please contact us with any questions or if clarification is needed. (507) 284-1050

Summary: Gross necropsy report was not submitted. This animal had chronic mesenteritis with acute small intestinal transmural ulceration. Foreign material and bacteria are observed on the periphery of the mesentery and are likely related to a rupture of the small intestine. Additionally, this animal had gastric ulcers and edema in the nonglandular stomach. Please see the report for details.

HISTOPATHOLOGY

Animal: 1	
cecum	There is serosal mesenteritis.
colon	no significant lesions
duodenum	There is serosal mesenteritis.
jejunum	Focally, there is a large transmural ulceration with hemorrhage and neutrophilic infiltrates. Multifocally, there is serosal mesenteritis.
kidney	There is multifocal tubular vacuolation.
liver	In the adjacent fat, there moderate mixed inflammatory cells (mononuclear cells-some pigment laden and lesser neutrophils) are a that encircle a few foreign bodies. There are perivascular pigment laden macrophages.
mesentery	The mesentery is markedly cellular and contains large areas of mucinous deposits and lesser hemorrhage and necrosis. Cellular infiltrates include mononuclear cells (some pigment laden), fibroblasts, mesothelial cells and lesser neutrophils and very rare multinucleated cell (chronic mesenteritis).On the periphery, there are foreign bodies and mixed bacteria (consistent with gastrointestinal contents). This material accumulation may the result of contamination at the time of cutting/processing tissue or the result of an acute intestinal rupture.
pancreas	There is serosal mesenteritis.
stomach	Multifocally in the nonglandular stomach, there is epithelial attenuation with loss of keratinization or ulceration and mucosal neutrophilic infiltrates.There is submucosal edema.There is serosal mesenteritis.

XIII. Eidesstaatliche Versicherung

Ich erkläre hiermit an Eides statt, dass ich die vorliegende Dissertation mit dem Thema:

The immune-modulating effects of PFKFB3 inhibition in a syngeneic ovarian cancer model

selbständig verfasst, mich außer der angegebenen keiner weiteren Hilfsmittel bedient und alle Erkenntnisse, die aus dem Schrifttum ganz oder annähernd übernommen sind, als solche kenntlich gemacht und nach ihrer Herkunft unter Bezeichnung der Fundstelle einzeln nachgewiesen habe.

Ich erkläre des Weiteren, dass die hier vorgelegte Dissertation nicht in gleicher oder in ähnlicher Form bei einer anderen Stelle zur Erlangung eines akademischen Grades eingereicht wurde.

München, den 25.10.2022 Assja Alexeevna Jeske